Fractal antennas and arrays: a review and recent developments

Anirban Karmakar (iD)

Department of Electronics and Communication Engineering, Tripura University (A Central University), Tripura, India

Abstract

In mathematical definition, a fractal is a self-similar subset of Euclidean space whose fractal dimension strictly exceeds its topological dimension which in turn involves a recursive generating methodology that results in contours with infinitely intricate fine structures. Fractal geometry has been used to model complex natural objects such as clouds coastlines, etc., that has space-filling properties. In the past years, several groups of scientists around the globe tried to implement the structure of fractal geometry for applications in the field of electromagnetism, which led to the development of new innovative antenna configurations called "fractal antennas" which is primarily focused in fractal antenna elements, and fractal antenna arrays. It has been demonstrated that by exploiting the recursive nature of fractals, several marvellous kinds of properties can be observed in antennas and arrays. The primary focus of this article is to provide a compressed overview of the developments in fractal-shaped antennas as well as arrays over the last few decades where the most prominent contributions mostly from IEEE journals have been highlighted. The open intention of this review work is to show an encouraging path to antenna researchers for its advancement using fractal geometries.

CAMBRIDGE UNIVERSITY PRESS

Introduction

Benoit Mandelbrot (1924–2010) was a French and American mathematician (Fig. 1) who referred himself as "fractalist" [1] and is well recognized for his contribution to the field of fractal geometry, who coined the word "fractal" and developed the theory of "roughness and self-similarity" in nature. As a visiting professor at Harvard University, Mandelbrot began to study fractals called "Julia sets" based on previous work by Gaston Julia and Pierre Fatou. In 1982, he expanded his ideas in "The Fractal Geometry of Nature" [1] which brought fractals into the mainstream of professional and popular mathematics. His informal and passionate style of writing and his emphasis on visual and geometric intuition made "The Fractal Geometry of Nature" accessible to non-specialists which sparked widespread interest in fractals which is acceptable in almost every field from finance to physics to medicine.

In the study of fractal structures, geometric series often arise as the perimeter, area, or volume of a self-similar structure. For example, the area of Koch snowflake [1] can be described as the union of infinitely many equilateral triangles (Fig. 2). Here, each side of the green triangle is exactly 1/3 the size of a side of the large blue triangle, and therefore has exactly 1/9 of the area. Similarly, each yellow triangle has 1/9 of the area of a green triangle, and so forth. Taking the blue triangle as a unit of area, the total area of the snowflake can be calculated as:

$$1 + 3\left(\frac{1}{9}\right) + 12\left(\frac{1}{9}\right)^2 + 48\left(\frac{1}{9}\right)^3 + \ldots\ldots \tag{1}$$

The first term of this series represents the area of the blue triangle, the second term represents the total area of the three green triangles, the third term represents the total area of the 12 yellow triangles, and so forth. Excluding the initial 1, this series is geometric with constant ratio $r = 4/9$. The first term of the geometric series is, $a = 3(1/9) = 1/3$, so the sum is:

$$1 + \frac{\frac{1}{3}}{1 - \frac{4}{9}} = \frac{8}{5}. \tag{2}$$

Thus, the Koch snowflake has 8/5 of the area of the base triangle leading to convergent series formulation.

Also, perturbation theory can be used efficiently to obtain a prescription that recursively generates the structure of the abstract attracter. This technique can be used in the calculation of the fractal dimension of the attracter of certain two- or three-dimensional maps. Presently, significant attention is being paid for characterizing the deterministic chaotic behavior of dynamic

where each copy is being transformed by a function system. IFS is based on affine transformation series, "w" which is defined by:

$$w\begin{pmatrix} x \\ y \end{pmatrix} = \begin{pmatrix} a & b \\ c & d \end{pmatrix} \begin{pmatrix} x \\ y \end{pmatrix} + \begin{pmatrix} e \\ f \end{pmatrix}. \qquad (3)$$

Here real number coefficients (a, b, c, d, e, f) are responsible for the movement of fractal elements in space: a, d – scaling; b, c – rotation by φ_1, φ_2 angles with respect to axis of coordinating system; and e, f – linear translation by the vector (e, f) respectively. These coefficients are expressed as follows: $a = \delta_1 \cos \varphi_1$, $d = \delta_2 \cos \varphi_2$, $b = \delta_2 \sin \varphi_2$, $c = \delta_1 \cos \varphi_1$. A canonical example is shown in Fig. 3 which is called Sierpinski Gasket [1] that begins with a triangle and the middle piece is cut out as shown in the generator in Fig. 3. This results in three smaller triangles for which the process is continued. The nine resulting smaller triangles are cut in the same way and so forth, indefinitely. The gasket structure is perfectly self-similar, with an attribute of many fractal images where any triangular portion can be seen as an exact replica of the whole gasket.

L-systems introduced by Lindenmayer in 1968 [2] is an albhabet based method which are used to describe the behavior of plant cells and to model the growth process of plant development. The recursive nature of L-system leads to self-similarity and fractal-like forms can also be described by L-systems. It is useful to create some fractals based on Hilbert and Peano curves.

A long-term effort by several researchers around the globe to combine fractal geometry with electromagnetic theory has led to a plethora of innovative antenna designs [2,3] which led to an era called fractal antenna engineering [4,5] which is primarily focused in two broad areas: the design of fractal antenna elements as well as the application of fractal to the design of antenna arrays. Fractal antenna geometries can be classified into two categories as deterministic and random. Random fractals are basically produced by the trajectories of non deterministic functions. Several studies on deterministic antenna structures for which the self-similarity property can be applied by a scaling factor have been carried out in this report. Several fractal geometries have been revisited for antennas with special characteristics, in the context of both antenna elements and spatial distribution functions for elements in antenna arrays.

In this review article, researches on fractal multiband antennas are summarized in section "Fractal antennas for multiband wireless applications". Section "Fractal antennas for wideband applications" embodies summaries of fractal wideband antennas. In section "Fractal antennas for UWB applications", fractal UWB antennas have been summarized and it concludes with a discussion on research trends in the field of fractal antenna arrays in section "Fractal array antennas".

Fractal antennas for multiband wireless applications

In modern scenario, a wireless device is often required to operate in more than one band of frequency. An antenna that covers multiple wireless communication bands is considered as a multiband

Fig. 1. Benoit Mandelbrot (Warsaw 1924–Cambridge 2010) considered as the father of Fractal Geometry [Wikipedia].
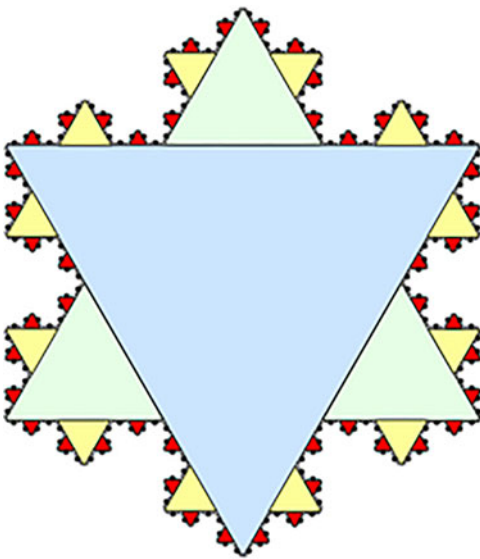

Fig. 2. Geometry of a Koch snowflake [2] [Wikipedia].

systems. The idea of characterizing the fractal quality of chaotic attractors in light of dimension-like parameters can be traced back to the geometric approach presented by Mandelbrot [1].

Based on Set Theory, Iterated Function System (IFS) [2,3] is a method for constructing fractals which are self-similar in nature. IFS fractals are made up of the union of several copies of itself

Fig. 3. Sierpinski gasket geometry till 4th iteration (0th, 1st, 2nd, 3rd, and 4th iteration) [2].
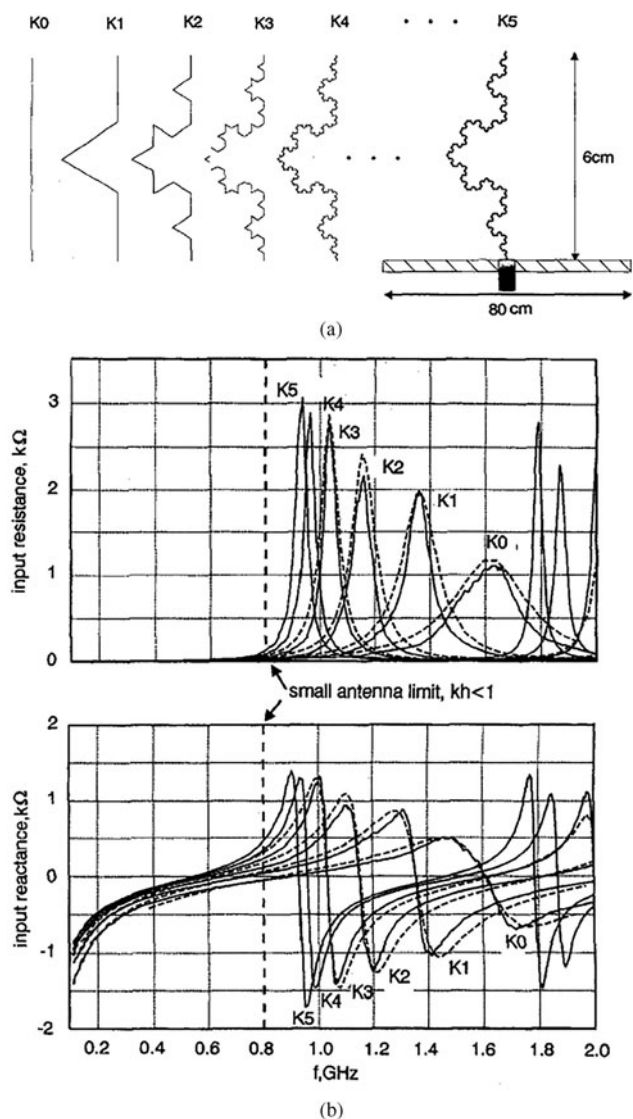
Fig. 4. (a) Koch monopole antenna with various iterations. (b) Variation of input resistance and reactance with the frequency of the antenna for different iterations [12].

Fig. 5. Fractal-tree dipole antennas [14].

antenna. This section revisited a few important works on fractal multiband antennas by various researchers. The application of fractal geometry for the design of wire antennas was first proposed in a series of articles by Cohen [6–11] which shows the fractalizing of the geometry of a standard dipole or loop antenna. Later, properties of Koch fractal monopole, investigated by Puente et al. in [12,13] have shown improved electrical performance over conventional linear monopole which is depicted in Fig. 4.

Monopole configurations with fractal top-loads have been considered here as an alternative technique for achieving size miniaturization. Puente et al. were the first to study a fractal two-dimensional (2-D) tree antenna which is inspired by a real tree where the top of every branch splits into more branches. It is seen that multiband behavior along with a denser band distribution than the Sierpinski antenna and the matched frequencies are found to be related to the length distribution over the fractal shape. Later, several antenna designs are considered [14] where fractal trees are shown to be as end-loads in order to miniaturize conventional dipole or monopole antennas (Fig. 5). Fractal
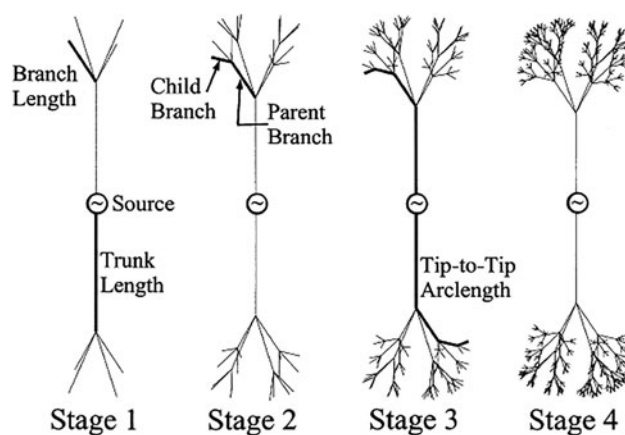
antennas are not limited to only wire antennas rather it provides a medium which is easy to analyze and fabrication.

In [15], a random 3-D fractal antenna (Fig. 6) with an electro-chemical deposition has been characterized by a monopole configuration. The novelty of this structure is the improvement of the impedance bandwidth compared to a similar 2-D fractal-tree antenna with less dense band distribution. In Fig. 6, f_i represents different resonant frequencies throughout the operating band.

Sierpinski triangle loop antenna with feed at the apex of the triangle [16] proposed by Karami and Karami, which has a radiation characteristic like a dipole. Electromagnetic characteristics of a Koch fractal antenna as an element and as an array are extensively examined by Deen et al. in [17] using MoM (Method of Moments). Sierpinski fractal planar monopole [18] antenna first reported by Puente et al. in 1996 which shows log periodic behavior in a single antenna itself with the number of resonances increasing with increasing iteration. Further studies on generalized antenna design based on Pascal Sierpinski gasket [19] which are derived from Pascal triangle showed log periodic behavior. In [20,21], Best showed that the multiband characteristics of the Sierpinski gasket are basically a function of the periodic placement of the four gaps located along the central vertical axis of the antenna. It is concluded that the electromagnetic nature of Sierpinski gasket is a function of the periodic arrangement of the four gaps positioned along the central vertical axis of the antenna, which results in Parany gasket antenna. He further studied on Parany gasket antenna (Fig. 7) with perturbed gaps which showed identical allocation of frequency bands along with multiband behavior.

From the design point of view, mathematical expressions given in [22] for the calculation of the frequencies of resonance of the Sierpinski gasket are found necessary. It is seen that multiple ring monopoles [23,24] have similar characteristics to the Sierpinski gasket monopole antenna. When the circular shape is changed to an elliptic, there is an improvement in the bandwidth and radiation properties. From the return loss plots, it is observed that the impedance bandwidth increases for higher resonance and the lower ones are not prominent. Perturbed Sierpinski gasket monopole antenna studied by Song et al. [25] is extensively studied for overcoming the matching difficulties of a perturbed Sierpinski gasket fractal antenna (Fig. 8). These techniques enables multiband matching to a conventional 50 Ω SMA connector, without using any kind of matching circuits. A methodology for reducing the frequency separation between the first and second band of these triangular antennas has also been proposed. Based on Sierpinski
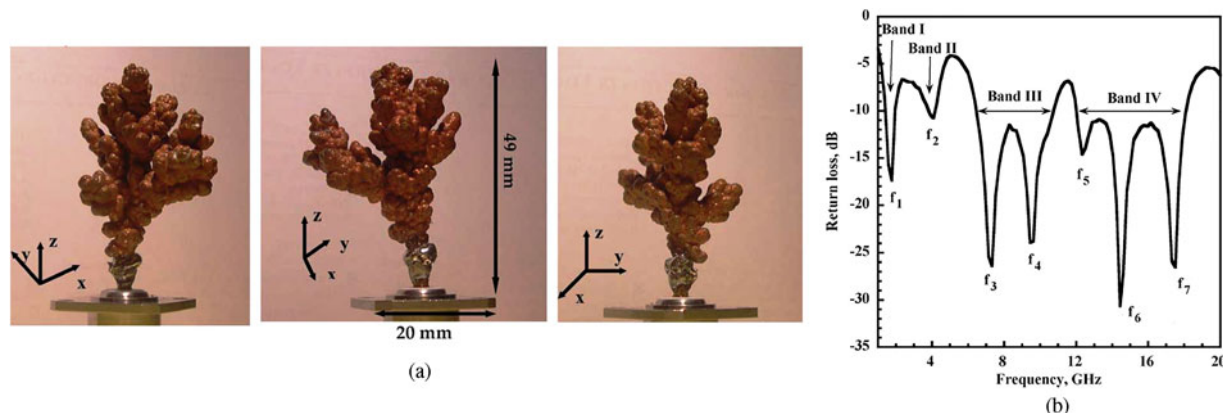
Fig. 6. (a) Fractal-tree monopole antenna. (b) Measured return loss characteristics [15].
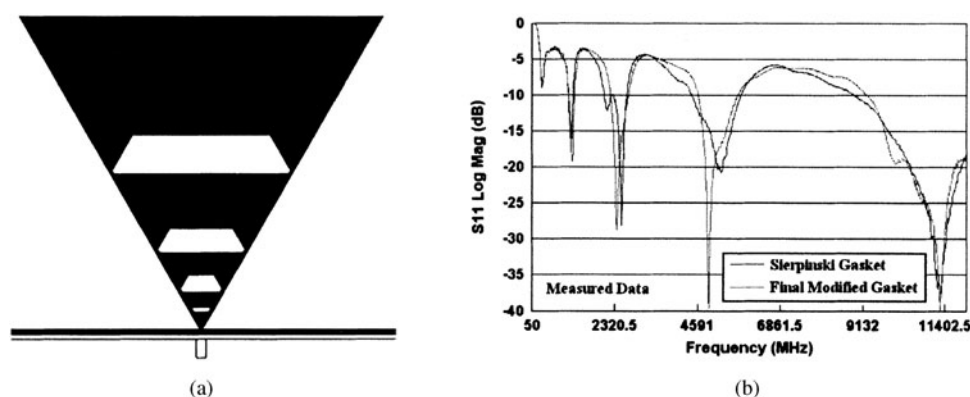

Fig. 7. (a) Perturbed Parany gasket antenna. (b) S_{11} characteristics compared to a conventional Sierpinski gasket monopole antenna [20].

gasket, a design for a triple-frequency broadband antenna based on a hybrid technique that combines a mono-band as well as dual-band broadband MPAs has been presented [26]. In [27], a perturbed Sierpinski fractal patch with slotted ground plane is employed in a modified version to achieve dual broadband characteristics which is shown in Fig. 9. The proposed antenna has two operational bands (808–1008 and 1581–2760 MHz) covering GSM/DCS/PCS/ IMT-2000/ISM/satellite DMB services.

An RF MEMS reconfigurable fractal antenna [28] on a flexible organic polymer substrate for multiband applications has been reported which operates at several different frequencies between 4 and 18 GHz. Here, three sets of RF MEMS (microelectromechanical systems) switches with different actuation voltages are used to sequentially activate as well as deactivate parts of a multiband Sierpinski gasket which allows direct actuation of the electrostatic MEMS switches through the RF signal feed. The antenna structure and measured S_{11} characteristics are shown in Fig. 10.

A dual-band fractal monopole antenna for handheld devices is proposed in [29] where a modified half-Sierpinski gasket is used in the patch to cover two wideband frequencies with bandwidths of 55% (1517–2670 MHz) and 16% (5135–5828 MHz) which is shown in Fig. 11.

A compact modified Sierpinski gasket monopole antenna with the ability to allocate both the 4 and 5.2 GHz ISM bands without a matching network is presented in [30]. Another modification of Sierpinski gasket (Fig. 12) is presented in [31] where a significant

size reduction is seen than a traditional Sierpinski gasket by controlling the space factor between the first two resonances. Results show that locating an internal antenna at the rear of the mobile handset minimizes radiation pattern alteration as well as gain depression due to the proximity of human tissue. It has an ability to handle both 4 and 5.2 GHz ISM bands without a matching network.

A dual-band compact PIFA (planar inverted-F antenna) implemented [32] using the conductive textile shield is proposed for wearable application. The antenna can be used both in the 45 GHz and in the 5.2 GHz bands with omnidirectional radiation characteristics with a measured gain of about 3.1 dBi. Based on first iterative fractal bowtie antenna design, recently a new buckled cantilever plate-based on-chip compact dual-band (60 and 77 GHz) antenna [33] using a CMOS compatible MEMS process has been proposed for efficient mm-wave applications (Fig. 13). It is vertically positioned with respect to the silicon substrate for better efficiency as compared to the horizontal position. An improved gain of 6 dB has been observed in simulation as well as in the measurement process of the antenna.

Another fractal geometry, which is well discussed by researchers in fractal antenna paradigm, is the Sierpinski carpet fractal (SCF). The SCF volume microstrip patch antenna is reported in [34] along with stacked SCF antenna over EBG (electromagnetic bandgap (EMBG)) ground plane. A multiband SCF antenna using transmission line feed is reported [35] with an impedance
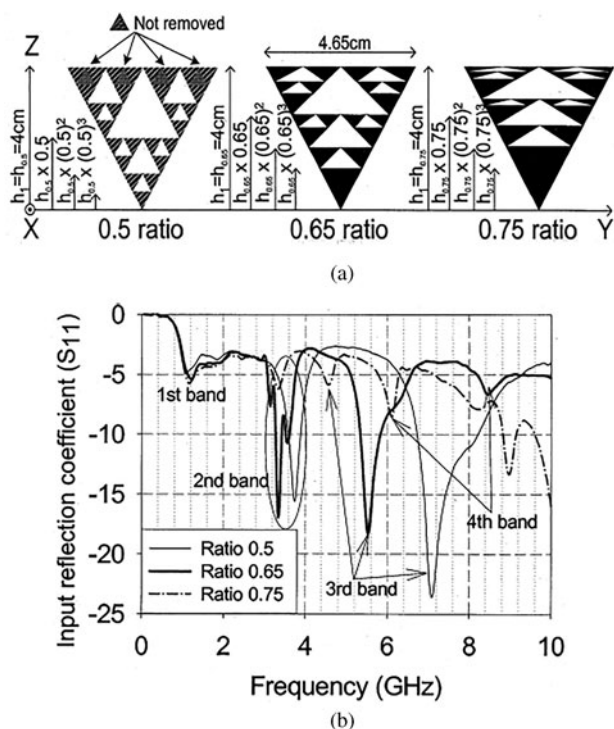
Fig. 8. (a) A perturbed Sierpinski monopole. (b) Corresponding S_{11} characteristics [25].

bandwidth of 47.1% at the resonant frequency of 7.93 GHz. In [36], a perturbed SCF planar antenna with CPW feed suitable for IEEE 8011a and 8011b lower and mid bands as well as for HiperLAN2 system is presented which is shown in Fig. 14. Another SCF patch antenna [37] with a slant strip in the first iteration is proposed for dual WLAN application. A fractal PIFA based on SCF is presented in [38] for mobile phone application. A printed dipole antenna [39] based on SCF has been reported for dual-band application with impedance bandwidths of 38.6 and 4.7% centered at 1.1 and 3 GHz. A novel microstrip patch antenna with a Koch prefractal edge and a U-shaped slot is presented [40] for multi-standard application in GSM1800, UMTS, and HiperLAN2. It is implemented in PIFA configuration with a size reduction of 62% (Fig. 15).

Taking the advantage of Koch profile, a dual-band antenna [41] is presented using reactive loading where the bandwidth is enhanced using a stacked parasitic technique. Another CPW-fed modified Koch fractal printed slot antenna is presented [42] for dual wideband characteristics suitable for WLAN and WiMAX. Here, the introduction of a Koch fractal slot lowers the frequency of operation along with wide-band matching. In [43], input impedances and radiation characteristics of half-wavelength Koch fractal V-electric dipoles having included angles 60°, 90°, and 120° have been discussed. Recently in [44], the introduction of partial Koch fractal boundaries to a traditional triangular patch results in antenna designs with high gain, low side lobe levels, and improved return loss. In [45], a Koch-like sided fractal bowtie dipole is presented which can operate in multiband as well as ultra-wideband regime depending upon notch angle φ. When this angle increases in the range 0°–90°, UWB transform into multiband gradually. Another tri-band antenna [46] which is end-loaded with Koch fractal loops is reported for radio frequency identification (RFID) applications. In [47], a multiband Fractal Koch dipole textile antenna is proposed for wearable applications.

Slot antennas in fractal domain are attracting much more attention in recent times. In [48], a third-order Hilbert slot antenna is reported with dual-resonance characteristics with a much smaller size to a printed half-wave dipole or full-wave slot antenna. Using Descartes circle theorem (DCT), a CPW-fed circular fractal slot antenna [49] is proposed for dual-band applications. In [50], a novel Spidron fractal slot antenna consists of a Spidron fractal slot, two microstrip feeding lines and a conducting reflector developed for multiband gap-filler application (Fig. 16). Here, two microstrip feeders are used to excite the Spidron fractal slot antenna at the 5 and 5.5 GHz frequency bands.

Some other types of fractal antennas are reported in [51], where a novel hexagon fractal corner-fed patch antenna in dipole configuration is analyzed that showed multi-band characteristics. A new type of fractal microstrip patch antenna named as the crown square fractal antenna is studied in [52]. Apart from showing multi-band characteristics and size reduction when compared to a near square patch antenna, these antennas are claimed to exhibit a pair of circularly-polarized bands in a wide VSWR bandwidth at high-frequency modes. A dual-band monopole antenna operating in the L1 and L2 GPS bands is presented in [53]. The Kock prefractal antenna has been synthesized by means of a

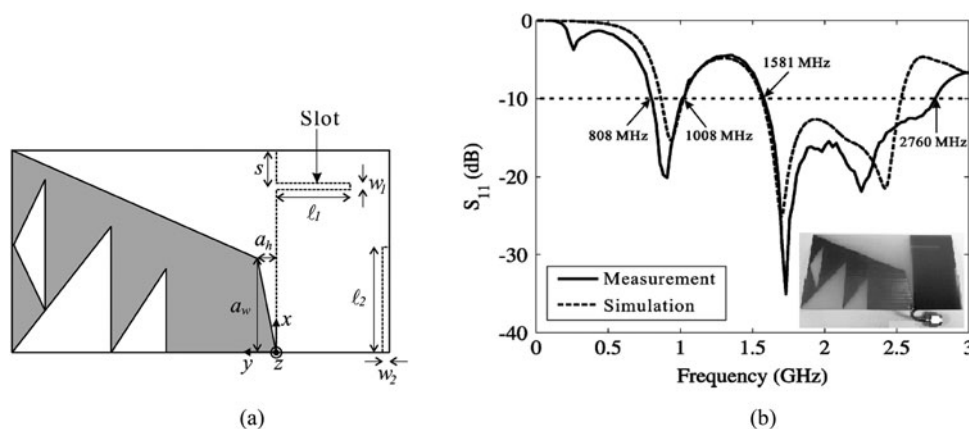**Fig. 9.** (a) Modified Sierpinski fractal patch with a slotted ground plane. (b) Simulated and measured S_{11} characteristics of the antenna with fabricated prototype (a_h = 5 mm, a_w = 25 mm, s = 8.7 mm, w_1 = 1 mm, w_2 = 1 mm, l_1 = 20 mm, l_2 = 28 mm) [27].
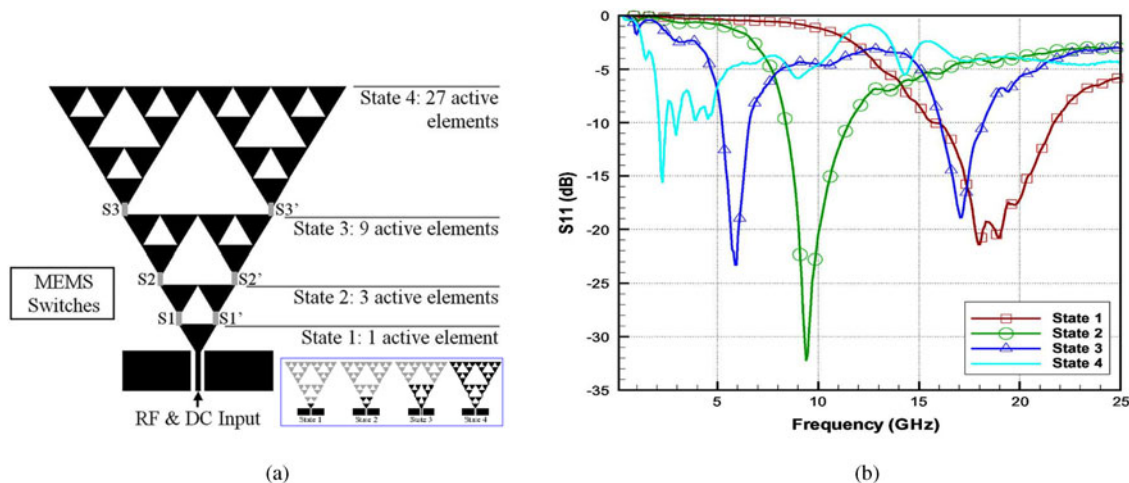
Fig. 10. (a) MEMS reconfigurable Sierpinski antenna. (b) Measured return loss characteristics of the proposed antenna [28].
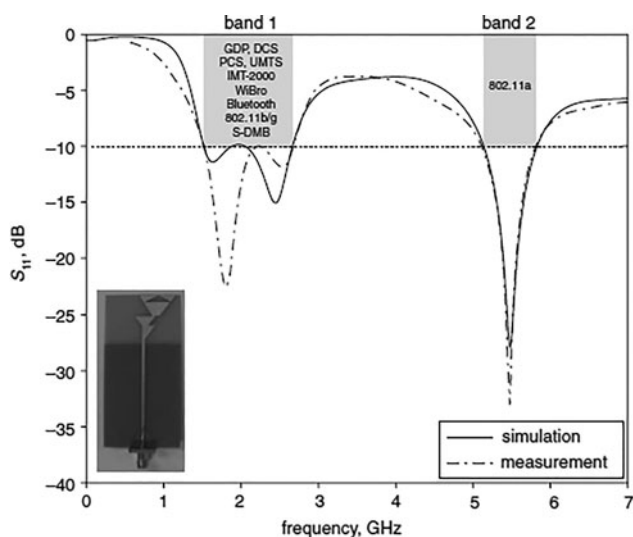

Fig. 11. Simulated and measured S_{11} characteristics of perturbed Sierpinski gasket monopole [29].

PSO for optimizing the values of the electrical parameters within the specifications. An alternative multiband approach [54] using Descartes theorem is presented for constructing a modified Sierpinski fractal monopole antenna where the resonances exhibit log periodic behavior. With increasing frequency, the patterns have an increasing number of lobes that exhibit array characteristic. Based on the Descartes theorem and non-constant fractal ratio, the multi-band performances of compound log-periodic Apollonian packing monopole antennas are presented in [55]. A triple-band patch antenna [56] working in *E5-L1* Galileo and WiMAX frequency bands is presented where the geometry of the antenna is defined by a Koch-like erosion in a Euclidian patch structure according to a Particle Swarm strategy.

A new type of fractal antenna [57] called hybrid fractal has been reported for multiband application which behaves similarly to the Sierpinski gasket, repeating its resonant frequencies by a factor of two. A rectangular fractal dipole antenna with two operating bands for RFID is presented in [58]. By using a fractal slot and metal meander patch, the proposed antenna has wideband as well as dual return loss characteristics. A multi-band Cantor fractal monopole antenna covering GSM, DCS, PCS, UMTS, and WLAN applications have been presented in [59]. In [60], several dual-band cavity-backed fractal aperture antennas are investigated where the problem formulation is done by using a hybrid finite element-boundary integral method. A triangular monopole antenna [61] on Sierpinski gasket fractal-based ground plane is proposed to obtain a dual-band characteristic for the 8011 standard (WLAN). It is observed that this fractal-based ground plane introduces new matched bands and can improve the existing ones. Based on real coded genetic algorithm in conjunction with electromagnetic simulations, a novel technique [62] for designing Sierpinski gasket fractal microstrip antenna is proposed. This method determines the side-length and the fractal iteration number of the antenna for the operations at 4.56, 7.51, and 11.78 GHz frequency bands. A monopole quad-band antenna based on a Hilbert self-affine prefractal geometry has been proposed in [63]. An innovative design of fractal monopole-like antenna [64] with five series of Hilbert-curve configuration is proposed for IEEE 8011a/b/g WLAN as well as circular polarization applications. A miniaturized triple-band planar antenna working in GSM and Wi-Fi frequency bands is described in [65] where a hybrid pre-fractal shape is obtained by integrating a Sierpinski and a Meander-like structure. A 2-D irregular fractal-jet printed antenna originated from a real image of a fractal jet fluid is designed [66] and characterized for 1–30 GHz multiband behavior. A modified fractal rhombic patch monopole multiband antenna [67] has been proposed for multiple wireless communication system. Here, a modified ground plane has been employed to improve input impedance bandwidth and high-frequency radiation characteristics. Another compact printed RFID dipole antenna is proposed [68] which consist of different combination of fractals with the aim of reducing antenna size. For the matching purpose with the essentially complex impedance of the electronic chip directly embedded into the radiator, a double T-match structure is used. Another hybrid design of a compact ring fractal monopole antenna [69] with semi ellipse ground plane is proposed for modern mobile devices having WLAN as well as WiMAX applications. By increasing the fractal iterations, very good impedance characteristics are obtained. A trapezoid monopole antenna [70] with quasi-fractal slotted ground plane is applied for dual-frequency applications where the dual
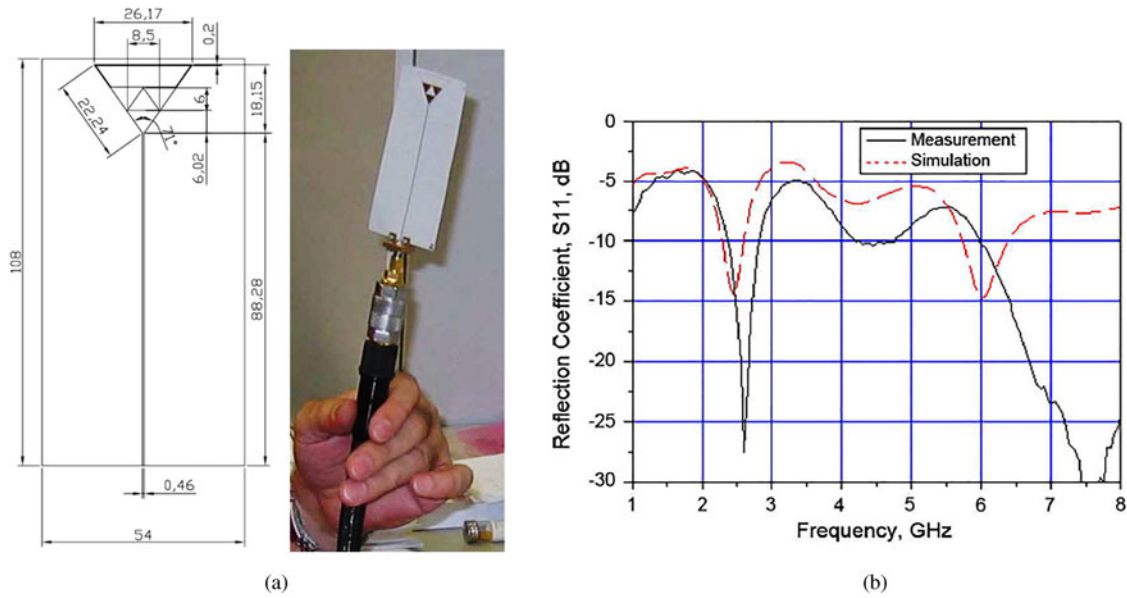
Fig. 12. (a) Numerical and physical model of the antenna [All dimensions are in 'mm']. (b) Simulated and measured S_{11} characteristics of the antenna [31].
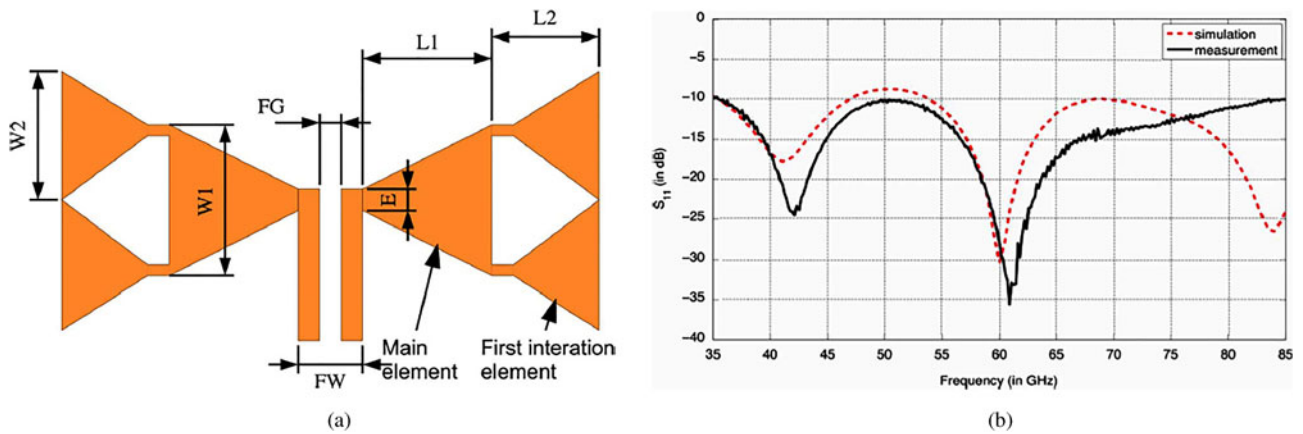
Fig. 13. (a) Antenna geometry ($L1 = 695\,\mu m$, $L_2 = 818.3\,\mu m$, $W_1 = 600\,\mu m$, $W_2 = 760\,\mu m$, $E = 25\mu m$, $FW = 60\,\mu m$, $FG = 10\,\mu m$). (b) S_{11} characteristics of the proposed antenna [33].
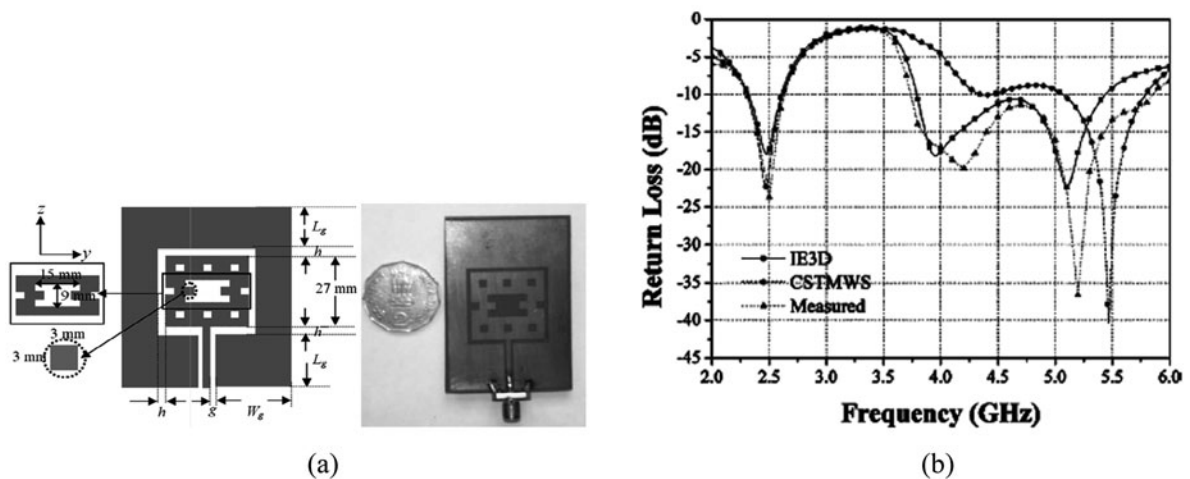
Fig. 14. (a) Dimension of the proposed antenna [g = 1 mm, Lg = 184 mm, h = 1.743 mm, Wg = 20.5 mm]. (b) Corresponding S_{11} characteristics [36].
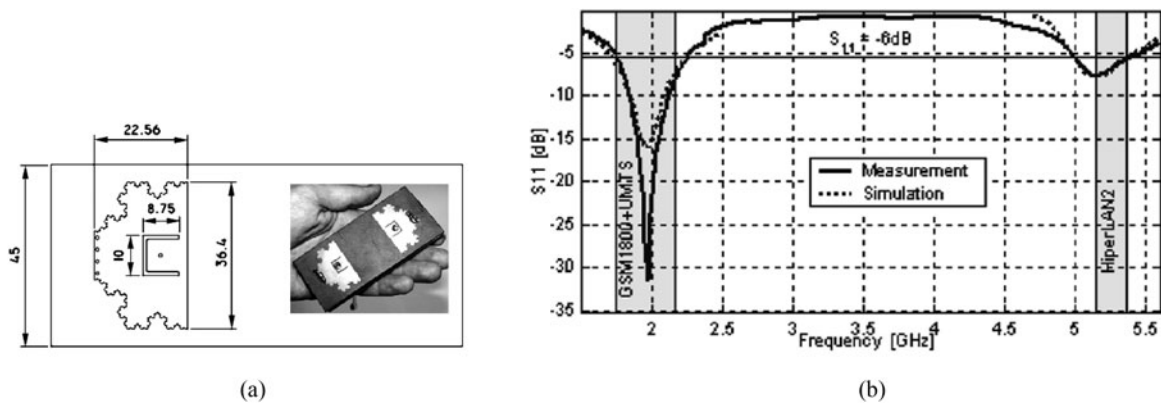
Fig. 15. (a) Koch curve fractal patch antenna with fabricated prototype in inset [All dimensions in 'mm']. (b) S_{11} characteristics of the antenna [40].
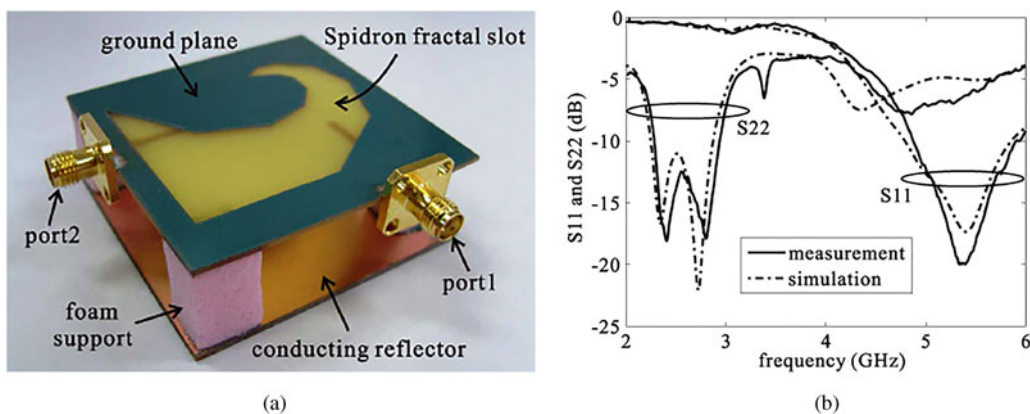

Fig. 16. (a)Fabricated Spidron fractal slot antenna. (b) Corresponding return loss characteristics. [50].
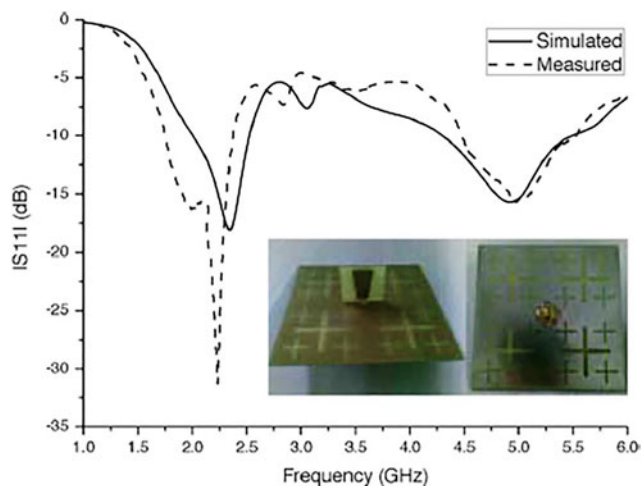

Fig. 17. Simulated and measured S_{11} characteristics of the antenna [70].

operating bands of the antenna are determined by the sizes of the radiator as well as the quasi-fractal structure (Fig. 17).

Here, quasi-fractal slotted ground plane is applied to improve the dual-band characteristics of the antenna. A compact dual-band circular polarized fractal antenna consists of a Hilbert-curve and self-complementary configuration is presented in [71]. This design combines the inductively loaded monopole antenna and the self-complementary antenna to obtain a new monopole antenna configuration. The Hilbert curve with a longer strip line determines the lower band of 43 GHz and the Hilbert curve with shorter strip line decides the higher band of 5.35 GHz. It is seen that by appropriately choosing the fractal properties [72], the design of a dual-frequency microstrip ring antenna using Minkowski curves can be done. A star-shaped fractal patch antenna is presented in [73] for miniaturization and backscattering radar cross-section reduction. A compact multiband third iterative E-shape fractal patch antenna [74] has been proposed for multiband application to achieve size reduction as well as to enhance the number of operating bands. This antenna operates on LTE/WWAN (GSM850/900/1800/1900/UMTS/ LTE2300/2500) band. A procedure [75] of planar antenna design using modal methods has been provided where the information about motif behavior is presented. By this method, it is possible to effectively analyze even complicated shapes like fractals. Here, the physical behavior of a planar antenna has been explained by modal decomposition along with a design of patch feeding and a full-wave analysis. It is seen that modal radiation patterns could successfully predict antenna radiation characteristics such as polarization or main lobe direction.

A design procedure is presented in [76] for making custom-made fractal antennas using artificial neural networks and the
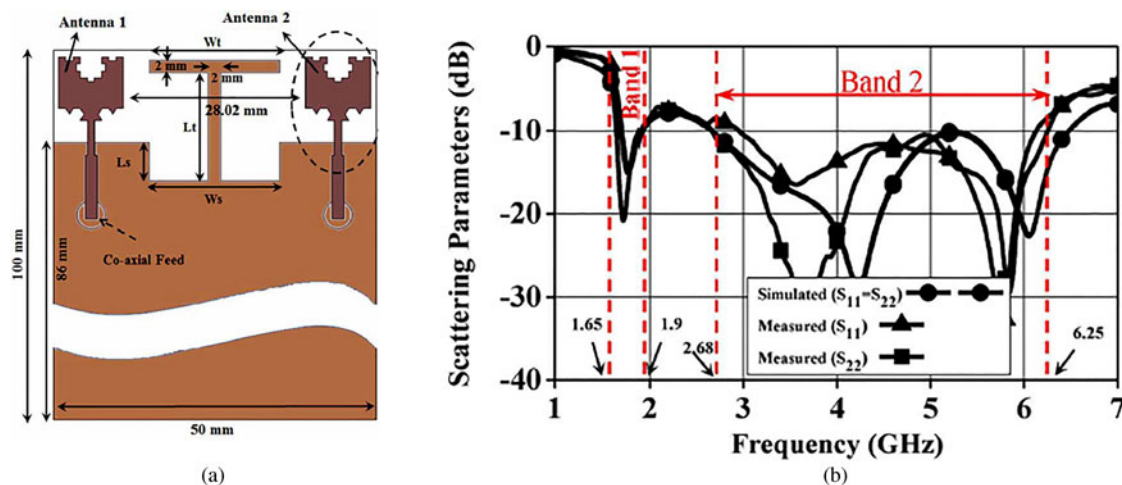
Fig. 18. (a) Geometry of the proposed antenna. (b) Simulated scattering parameters of the antenna [83].

particle swarm optimization (PSO) considering Sierpinski gasket and Koch monopole antennas. Based on a perturbed planar Sierpinski fractal shape, a dual-band monopole antenna suitable for Long Term Evolution (LTE) standard is proposed in [77] where the antenna geometry has been determined by means of a PSO. A compact modified Minkowski fractal loop monopole [78] antenna is proposed for USB dongle applications which cover Wi-Fi (4–484 and 5.15–5.35 GHz) and WiMAX (5–7 and 3.4–3.6 GHz) applications. Another compact microstrip antenna with a combination of square and Giuseppe Piano fractals [79] has been proposed for multiband operation along with circular polarization. Good axial ratio (AR) and radiation patterns prove the effectiveness and suitability of the proposed approach for wireless applications. A dual-band antenna obtained by replacing a segment of a square ring microstrip antenna with fractal Minkowski curve is studied in [80]. By increasing the indentation factor of the fractal radiator, the resonance frequencies of the antenna can be changed and by suitably optimizing this value, antenna can be designed with improved bandwidth with good gain at both the resonance frequencies. A dual-band microstrip RFID reader antenna [81] with tree-like fractal resonator is designed with 4.4 and 3.1% BW, respectively. Tri band RFID antennas [82] are proposed for RFID reader as well as RFID tag for using in logistics management, traffic toll collection, and tago-metry. Based on Minkowski island curve and Koch curve fractals, a hybrid fractal planar monopole MIMO antenna (Fig. 18) has been presented in [83] which provides band widths of 14% for band-1 (1.65–1.9 GHz) and 80% for band-2 (68–6.25 GHz).

A pseudo-self-complementary four-stage Parany monopole with side triangular complements and side-notched vertices has been proposed in [84] for multiband applcations. This antenna has a smaller physical area and length than the traditional Parany monopole. In [85] a compact low-profile circularly-polarized (CP) antenna has been examined based on the combin-ation of fractal metasurface and fractal resonator. A CPW-fed multiband fractal slot antenna [86] loaded with a dielectric reson-ator for multiband wireless applications is proposed. Here the Minkowski fractal geometry is used to generate multiband behav-ior as well as helped in miniaturization than its Euclidian counter-part. In [87], a circularly-polarized compact microstrip antenna using Koch fractal geometry for UHF RFID system is presented. A novel DRAF geometry is introduced in [88] and implemented

on an equilateral triangular patch for antenna miniaturization while keeping the bandwidth of the antenna constant. In [89], it is seen that the use of fractal DGS in the design of L-band pla-nar antennas gives better antenna performance as compared with antennas without DGS (defected ground structure) and antennas with traditional DGS. In [90], a multiband antenna has been pro-posed to function as a receptor element in radio-frequency energy harvesting applications. In [91], the design of a dual-band wear-able fractal-based monopole patch antenna integrated with an EBG structure is presented which covers the GSM-1800 and ISM-2.45 GHz bands. A multiport sharing compact antenna is presented in [92] where the radiator is composed of two Sierpinski fractal triangles. These two main ports have the oper-ating band of 1–4 GHz where the auxiliary port with a multiband at around 2.4, 3.4, and 5.2 GHz provides an additional WLAN/WiMAX port. In [93], a novel single-radiator card-type tag antenna is proposed using a series of Hilbert-curve loop and matching stub for HF/UHF dual-band RFID application. By mer-ging the series Hilbert-curve HF coil along with square loop UHF antenna, a single radiator of RFID tag is obtained that meets the requirement of compactness and HF/UHF dual-band operation as shown in Fig. 19.

In [94], a sensor for a Moore fractal antenna is proposed to detect partial discharge (PD) in gas-insulated substations that can work at an ultra-high frequency. In [95] a low-cost, frequency-agile triangular Sierpesnki gasket-based antenna is pro-posed for use by wireless sensor nodes in IoT applications. The antenna consists of PIN diodes, inductors as well as a single bias line to switch between two modes of operation. By switching the diodes on or off, the desired frequency agility between UHF (800 MHz) and the WLAN band (2400–2500 MHz) is achieved with corrosponding bandwidths of 200 and 1000 MHz, respect-ively. The concept called additive manufacturing techniques for the fabrication of 3-D fractal monopole antennas is presented in [96]. The 3-D designs based on the Sierpinski fractal concept is studied and discussed. In [97], a single-feed circularly-polarized antenna is presented where the CP radiation is achieved by adjust-ing the dimension of the fractal defected ground structure (DGS). In [98], a rectenna topology is presented by using a compact frac-tal patch antenna with the rectifier circuit that is integrated into the same physical structure suitable for harvesting and wireless power transfer applications. In [99], a single patch antenna is
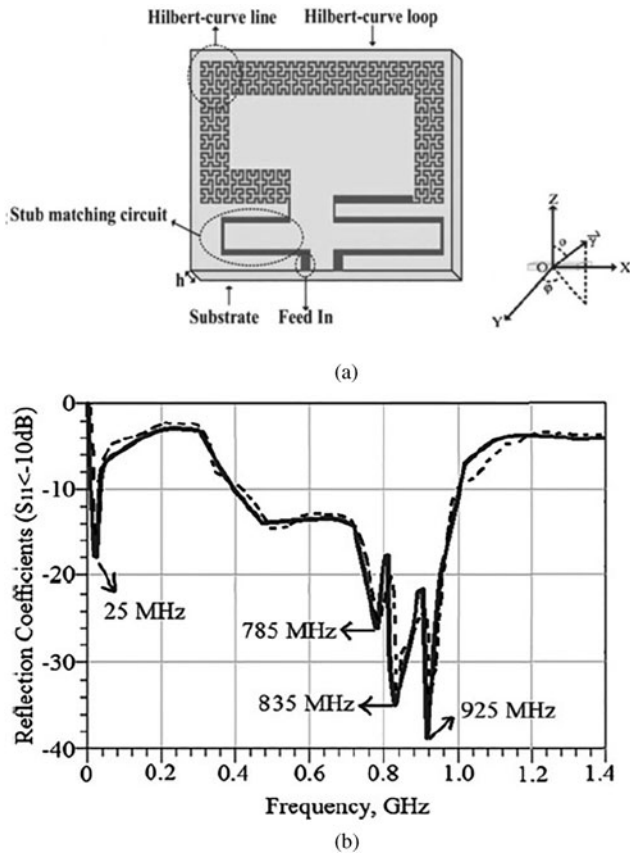
Fig. 19. (a) Geometry of the proposed antenna. (b) Return loss characteristics of the antenna [93].

Hilbert curve monopole antenna is designed with operating bands at WLAN 2.4, 5.8 GHz, Wi-max 3.5, 5.5 GHz, and RFID 5.2 GHz. In [102], an spiral antenna with a new fractal reflector for short-range sensing has been proposed to improve some features of the equiangular and Archimedean spiral antenna.

In [103], it is shown that SRRs can be applied for better impedance matching which can improve the bandwidth of a fractal antenna. This theory is successfully verified by designing a multiband circular fractal antenna which is loaded with SRRs, and the results have been compared for both the cases. The antenna shows improved impedance matching at all resonant frequencies. In [104], for the proposed fractal antenna at each stage, a new modified square patch with a half size of that used in the previous stage is added to shape the dual fractal-structure antenna which is shown in Fig. 20.

The antenna has dual-band characteristics that meet the specifications of the wireless fidelity Wi-Fi and WiMAX applications. The antenna also achieved an AR bandwidth (3 dB) which is 35% of the first operating band and 30% of the second operating band. In [105], an investigation is conducted on Hilbert metamaterial printed antenna to realize the possibility of organic materials usability in radio frequency (RF) electronics for RF-energy harvesting. A complementary stacked patch antenna based on Sierpinski fractal is introduced in [106] where it is seen that this new complementary structure enhances the antenna performances, retaining the basic characteristics of the Sierpinski antenna. Stacked patch antenna is proposed in [107] where fractal shaped defects have been etched from the patch surfaces which produce dual-band characteristics as well as size reduction. Based on Sierpinski gasket fractal, an electromagnetically coupled multilayer equilateral triangular stacked patch antenna is proposed in [108] for dual-band characteristics. Another stacked patch antenna consisting of a second iteration Minkowski-island-based (MIB) fractal patch is presented [109] for unidirectional radiation applications with 39.1% size reduction. It produces AR band width of 44 GHz. Based on complementary MIB fractal geometry, an aperture coupled stacked fractal patch antenna [110] has been presented with circular polarization. Dual-band responses at 3.5 and 5.25 GHz are obtained with 3 dB AR bandwidths of 1.4 and 0.76%.

In this section, we have provided an overview of recent developments on fractal multiband antennas where it is evident that

proposed to achieve the same directivity as an array with an equivalent area but without using the complex feeding network. In [100], a CPW-fed reconfigurable antenna using crescent-shape fractal geometry is presented where the frequency reconfigurable approach is obtained by using RF PIN diodes, resistor, and inductors. The design allowed the reconfigurable switching up to eight frequency bands between 1.46 and 6.15 GHz. In [101], a novel multi-band microstrip line-fed metamaterial-based bisected
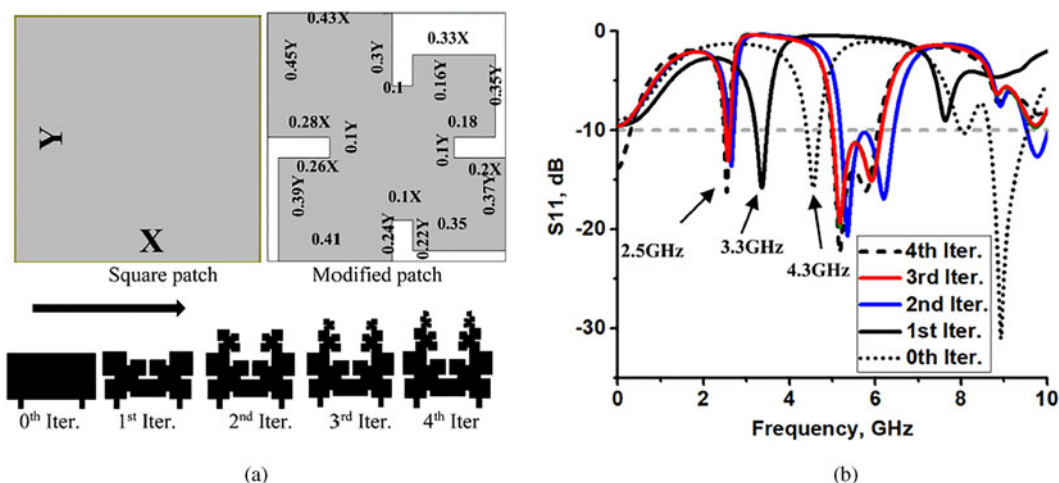

Fig. 20. (a) Configuration of the proposed antenna. (b) Return loss characteristics of the antenna [104].
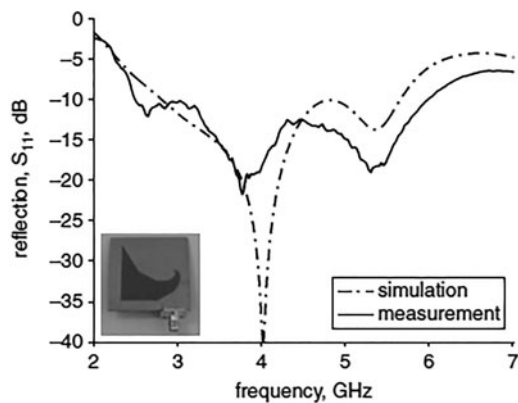
Fig. 21. Simulated and measured return loss of the antenna [117].

several fractal geometries can be efficiently explored for antennas with multiband applications because a fractal can fill the space occupied by the antenna in a more effective manner than traditional Euclidian antennas that leads to more effective coupling from feed to free space in less volume.

Fractal antennas for wideband applications

The demand for today's wireless communication systems is not only a compact antenna but also an antenna with a large band width to provide several services in a single device. Wideband antennas can cover sufficiently large operating frequency bandwidth for many applications with a relatively large form factor. It is seen that besides achieving miniaturization and multiband nature, fractal concept can also be effectively explored to achieve wideband characteristics.

Using the concept of DCT [111] and self-similar iteration design; circular fractal antennas are proposed which exhibit frequency-independent characteristics and multiband spectra. In [112], a new uniplanar self-similar structured wideband loop antenna is presented where by alternating an inverted matrix sequence, wide impedance bandwidth has been obtained from 2 to 20 GHz for VSWR <5. Another novel wideband and compact fractal Kokh antenna is proposed [113] which has smaller size and wideband behavior respect to similar fractal Kokh antenna

designs. The proposed antenna is able to achieve an impedance bandwidth of 19% for VSWR <2. . A compact wideband snowflake fractal antenna is proposed where various iterations with probe feed and capacitive coupled feed are compared and an optimized design is presented in [114]. It is shown that, with an airfilled substrate and capacitive feed, an impedance bandwidth up to 49% can be obtained. A planar Koch fractal loop antenna with broadband characteristics is presented in [115] where the CPW feed along with radial stub makes the antenna completely planar which can be integrated with other microwave circuits. In [116], a new planar fractal antenna using third iterative Penta-Gasket-Koch (PGK) has been introduced where the matching performance of planar PGK has been compared with that of conventional PGK monopole antenna. This design achieved a good input impedance match and linear phase throughout a wide operating band of 1.5–20 GHz (<−5 dB) along with satisfactory time-domain performance. A broadband circularly-polarized fractal antenna [117] is proposed (Fig. 21) where the concept of a novel Spidron fractal is employed to achieve both broadband as well as circular-polarization characteristics.

Printed slot antenna with a fractal-shaped square wide slot for bandwidth enhancement is proposed in [118] where the impedance bandwidth is 3.5 times that of the corresponding conventional printed microstrip line-fed wide-slot antenna. It is shown that the proper selection of iteration factor and iteration order of the fractal shape improves the impedance bandwidth significantly (Fig. 22).

Sierpinski carpet (SC)-based square monopole antenna [119] has been designed using the possibilities of the metalized foam technology. In terms of impedance bandwidth, the reflection coefficient is <−7.7 dB from 824 MHz up to more than 6 GHz having a total average efficiency of 79%. In [120], a compact second iteration SC fractal shape antenna is presented with the combination of the planar CPW-fed and the conventional monopole-fed antennas. This technique can provide a very good improvement in parameter magnitude considering SC geometry throughout the 4.65–10.5 GHz band pass. In [121], a Sierpinski fractal-shaped slot is employed for a wideband operation covering from 1.96 to 3.78 GHz. Here, the lower edge of the operating frequency band of the slot antenna is lowered by the fractal technique which results in a compact design. Another wideband antenna operating in a portion of the L-band frequency range is presented in [122]
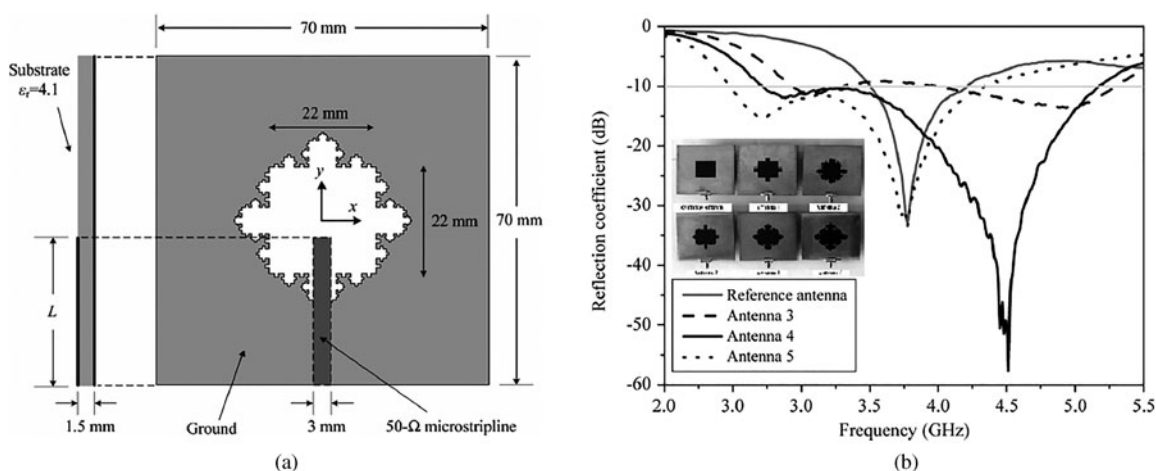

Fig. 22. (a) Geometry and dimension of the proposed slot antenna. (b) Measured S_{11} characteristics at different iterations [118].
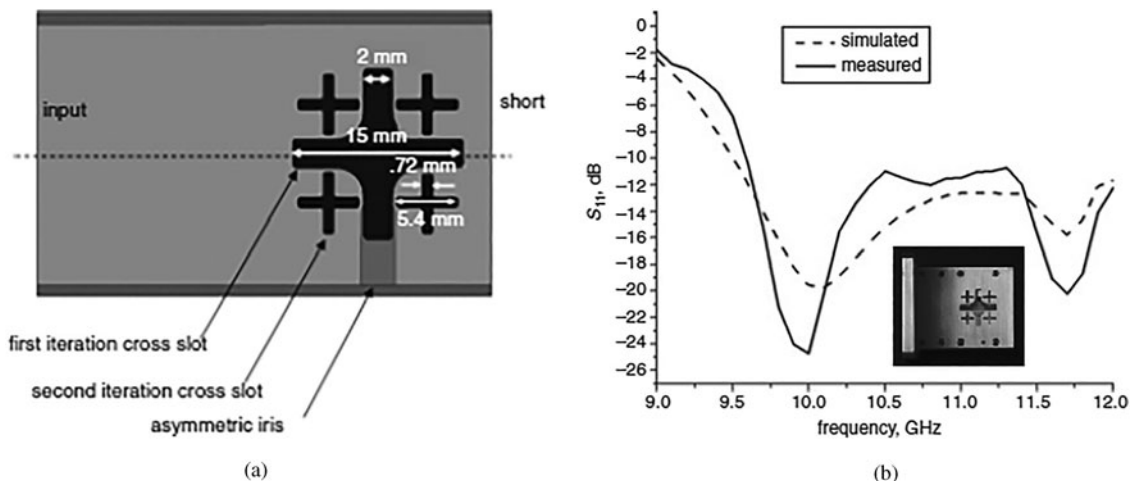
Fig. 23. (a) Layout of cross dipole fractal-shaped slot antenna. (b) Simulated and measured S_{11} characteristics of the proposed antenna [123].

which is based on a Julia prefractal geometry and also optimized by means of hybrid-coded genetic algorithm to minimize size and VSWR ratio. A new fractal patterned iris-loaded cross dipole slot antenna along the broad wall of a rectangular waveguide at X-band is presented in [123] for wideband operation (Fig. 23) where tapering the junction of the cross slots results in wide impedance matching. It is seen that bandwidth enhancement better than 2 GHz is achieved with the optimization of iris depth along with the inclusion of a second iteration slot in the vicinity of the primary cross slot.

In [124], a study on dielectric resonator antennas (DRA) with fractal cross-sectional areas has been investigated. Two main configurations of these novel types of DRA have been investigated. Analyses of these proposed DRAs are performed numerically using the finite element method and verified by the finite integration technique and a good agreement between the methods is found. In [125], a CPW slot loop-fed Minkowski-shaped fractal DRA is proposed (Fig. 24) which exhibits a fractional bandwidth of 64% (5.52–10.72 GHz) and a maximum gain of 4.9 dBi. It is highlighted that electrical boundary lowers resonance frequency, whereas fractal magnetic boundary increases the resonant frequency. It is concluded that the Minkowski fractal DRA provides the widest impedance bandwidth along with stable gain amongst the other proposed geometries.

Recently, a compact hemispherical DRA [126] based on Apollonian gasket geometry is proposed where the fractal geometry exhibits a wide impedance bandwidth of 47% at a resonant frequency of 3.6 GHz. However, from this study, it is seen that other than conventional planar monopole antennas, fractal slot antennas and recently DRA has emerged as a good candidate in wideband antenna paradigm. In [127], a circularly-polarized Spidron fractal dielectric resonator antenna is presented where a wide AR bandwidth (3 dB) is realized by merging a Spidron fractal dielectric resonator and a C-shaped slot that can produce circular polarization characteristics. A novel dual-broadband DRA (DRA) (Fig. 25) is presented in [128]. This proposed antenna consists of both dual-band and wide-band features by the use of modified Sierpinski structure.

The measured impedance bandwidths are 2.25–2.6 GHz (14.46%) and 3.1–4.1 GHz (27.78%), which can cover WLAN and WiMAX, 3.4–3.69 GHz bands. Stable radiation patterns and gain of about 5 and 3.8 dBi at 2.4 and 3.5 GHz have been observed. A novel fractal AMC structure suitable for the low-profile wideband antenna is presented in [129] where the ±90° reflection phase bandwidth is from 1.1 to 3.03 GHz. A broadband fractal antenna for positioning applications for handheld devices and sensor nodes is proposed in [130]. The antenna shows a measured VSWR bandwidth of 400 MHz (1.37–1.77 GHz) and AR
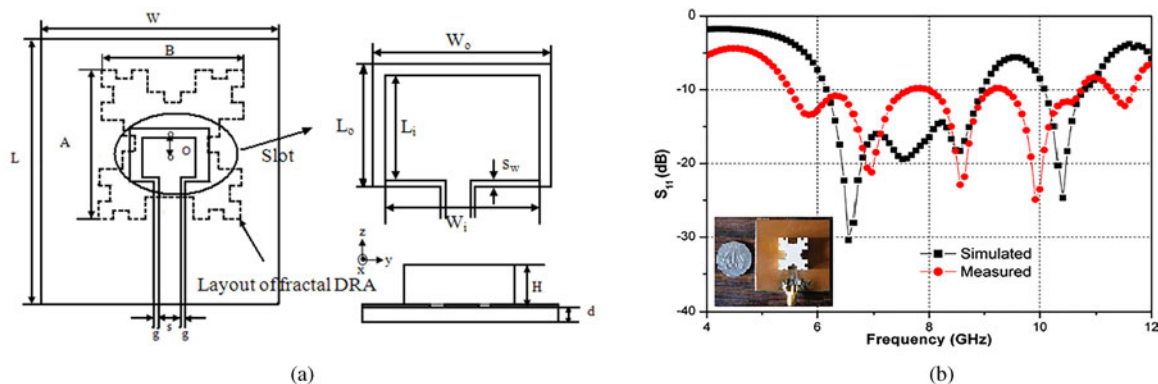

Fig. 24. (a) Configuration of the proposed antenna along with top view and side view [L = W = 50 mm, L0 = 10 mm, W0 = 11 mm, Li = 6 mm, Wi = 8 mm, Sw = 0.3 mm, O = 0 mm]. (b) Simulated and measured S_{11} of the fractal DRA [125].
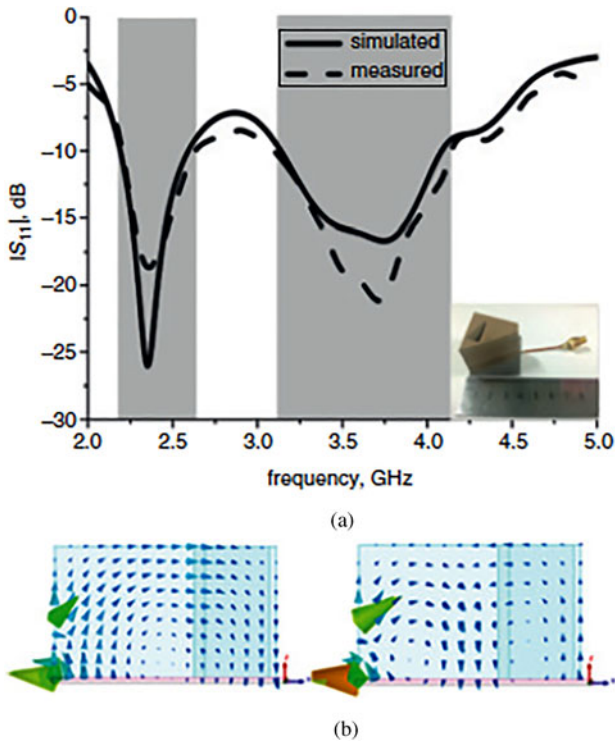
Fig. 25. (a) Simulated and measured S_{11}. (b) E-field distribution at 2.4 and 3.5 GHz [128].

A fern-leaf inspired antipodal Vivaldi fractal antenna (AVA) is presented in [135] which provide a fractional bandwidth of around 175% (Fig. 26). The antenna can radiate maximally in end-fire direction with less directivity at lower frequencies. In [136], the design of a flexible fractal EBG evaluates its performance impact on a wearable CPW antenna in the frequency range 20–40 GHz. A novel fractal AMC with a bandwidth of 5.1–7.4 GHz (36.5%) is applied [137] in a monopole antenna as a back-cavity for low profile and radiation performance improvement. A miniaturized hexagonal-triangular fractal antenna is presented in [138] for wide-band applications that offered the bandwidth of 3–25.2 GHz. A new approach has been proposed in [139] for improving the gain, directivity, and bandwidth of a conventional AVA. Inserting a fractal-shaped parasitic lens in the antenna aperture and fractal-shaped dielectric lens in the radiation aperture of the antenna is found to be an effective approach without compromising the size of the antenna. In [140], a fractal decoupling structure is proposed for suppressing the mutual coupling of the vehicular PIFA antenna array with a small center-to-center distance of $0.17\lambda_0$. In [141], an inkjet-printed tree-shaped fractal antenna with a small metal footprint is presented along with its method of fabrication on a flexible substrate. In [142], a low-profile semi-cylindrical multilayer fractal DRA with rotation, for super-ultra-wideband applications, is proposed where a compact multilayer cylindrical segment fractal structure based on the stacking approach is used for BW enhancement. In [143], the paper proposes a compact Sierpinski fractal-inspired DRA based on square- and pyramidal-shaped perforations which can be used for wideband as well as high gain applications. The antenna has a maximum gain of 6.56 dBi with a wide bandwidth of 5.2 GHz which is suitable for C-band and X-band applications.

Fractal wideband antenna is an emerging field that employs fractal concepts for its self-similarity and space-filling property. This unique feature of fractals allows antenna designers to design antennas with wideband characteristics into a compact physical space. It is observed that most fractals have complicated shapes with many corners such that their discontinuity enhances the bandwidth and effective radiation characteristics of antennas.

bandwidth of 360 MHz (1.47–1.83 GHz). In [131], a design of a wide band Hilbert fractal antenna for the purpose of detecting and classifying different common PD types in an oil-paper insulated system has been demonstrated. A wideband frequency reconfigurable Koch snowflake antenna was presented in [132] where the proposed antenna is feasible for use as an array element due to its compactness (at 2.9 GHz). In [133], an embedded dual-element and small-size RDRA is presented where the use of fractal geometry and the generator sector formats for Minkowski and Sierpinski to convert rectangular dielectric antenna to its fractal counterpart for bandwidth enhancement. In [134], a compact wideband ultra-high-frequency antenna is developed by applying Minkowski fractal geometry on both the lateral boundaries of monopole and the upper boundary of ground plane as well as loading the asymmetric strips at the top of monopole by which the miniaturization is realized.
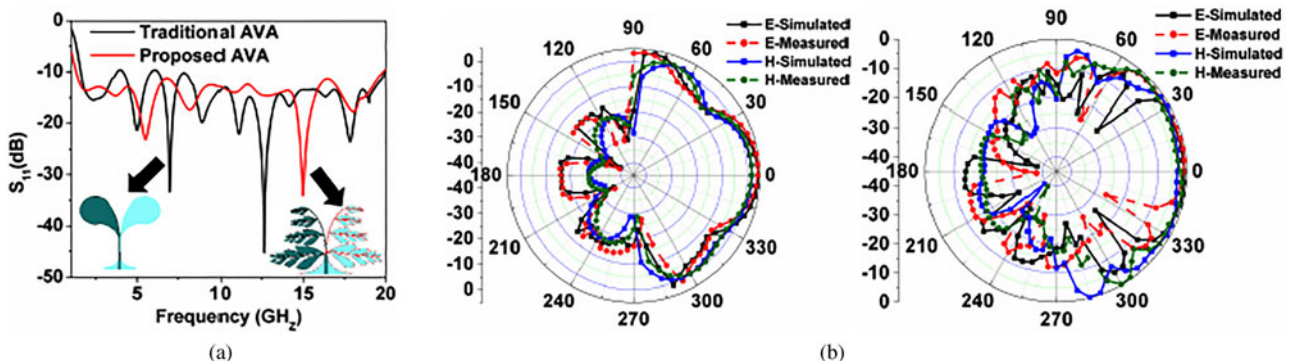
Fractal antennas for UWB applications

The adopted term ultrawideband (UWB) in 1989 by the US department of defense has re-emerged the century-old concept for modern day wireless applications. The release of the 7.5 GHz unlicensed spectrum in the year 2002 by the US Federal Communications Commission [144] for commercial

Fig. 26. (a) Simulated S_{11} characteristics of the proposed antenna. (b) Radiation patterns of the antenna at 12 and 20 GHz [135].

usages sparked a renewed interest of UWB in industries, academics, and governments. In the late 1950s and early 1960s, a family of wideband antennas was developed by Rumsey *et al.* [145] which was classified as a class of frequency-independent antennas or wideband antennas. Later, numerous radiators with different topologies, architectures, and various types of feeding are created [146] to obtain wider bandwidth. Among them, many researchers studied on UWB which are specially concentrated on fractal-based antennas because they possess not only small size, light weight, and thin shape for portable devices that have a rigorous limitation of space, but also wide bandwidth and good radiation characteristics.

Fractal was introduced first by Lui *et al.* [147] in UWB, where by employing a fractal-shape tuning stub; good impedance matching as well as flexible band-notched function is achieved. A printed slot antenna is proposed in [148] where by introducing a Koch fractal slot, not only the size of the antenna is significantly reduced but also a band notch characteristic has been achieved. A compact CPW-fed UWB circular fractal [149] antenna has been proposed which provides good UWB performance. An apollonian fractal-shaped UWB circular monopole antenna [150] based on DCT is presented where different self-similar geometries from DCT are analyzed and optimized for UWB applications. In [151], it is shown that different fractal geometries may be combined at a time for the design of UWB radiators. Here a monopole square patch antenna is introduced by shaping its edges into the form of a Giuseppe Peano fractal and its surface area as an SCF.

A novel modified microstrip-fed UWB printed Pythagorean tree fractal monopole antenna (Fig. 27) is proposed in [152]. Here, by inserting a modified Pythagorean tree fractal in the conventional T-patch, a wider impedance bandwidth along with new resonances are produced. In [153], a compact fractal binary tree band notched slot antenna is presented and demonstrated for UWB radio. Here, by etching a dual band-notched resonance compact slot using a fourth iteration fractal binary tree, two additional filters have been applied to the antenna which reduces
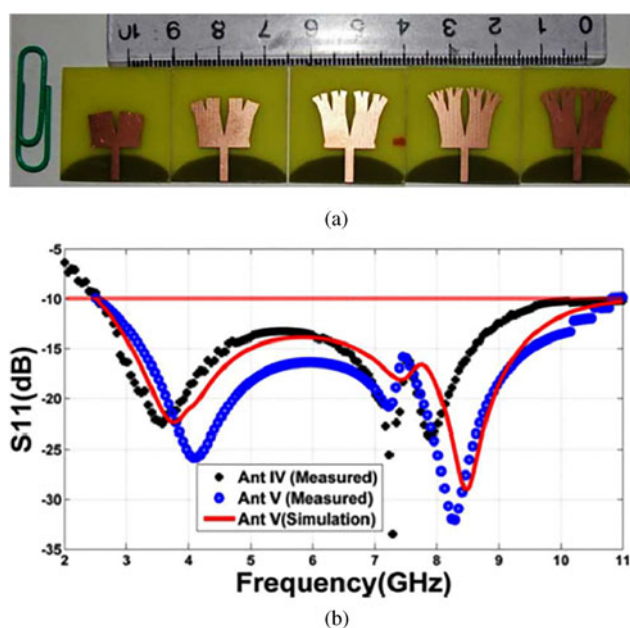
interference to other legacy bands. A CPW-fed wide slot antenna using Cantor set fractal technology has been presented in [154] for UWB applications. Here, the impedance bandwidth is widened by inserting two symmetrical triangular tapered corners at the bottom of the rectangular wide slot. A new approach for the design of a planar monopole UWB antenna is proposed in [155] to achieve a good impedance matching and stable omnidirectional radiation characteristics. Here, two compact antennas with circular ground and fractal ground is presented to overcome the drawbacks of a conventional UWB monopole antenna. A design of a novel and compact UWB fractal-based monopole antenna is reported in [156] where the enhancement of the antenna's bandwidth is achieved by increasing the unit cells of the fractal tree without significantly impacting antenna's physical dimension. Some paper-based inkjet-printed UWB fractal antennas are presented in [157] where it is demonstrated that applying is a successful method for reducing fabrication costs in inkjet-printed antennas, while retaining or enhancing printed antenna performance. A compact CPW feed planar monopole antenna is proposed in [158], comprising a fractal radiating patch in which a folded T-shaped element (FTSE) is embedded (Fig. 28).

The impedance matching of the antenna is determined by the number of fractal unit cells and the FTSE which provides the necessary band-notch functionality. An investigation on multi resonance technique to achieve UWB characteristics in a CPW-fed monopole antenna is presented in [159]. It is found that by addition of small fractal elements at the corners of a polygon patch, standard UWB bandwidth can be covered while maintaining compact antenna dimension.

Besides exploiting the frequency band of 3.1–10.6 GHz for ultra-wideband applications, the present users of wireless communication technology are eagerly searching for a super-wideband (SWB) antenna to cover both the short- and long-range communication for ubiquitous applications. Usually, an antenna with the bandwidth ratio larger than 10:1 for impedance bandwidth at 10 dB return loss is called SWB [160,161]. In this section, some fractal-based SWB antennas are reviewed.

Based on an iterative octagon, a new SWB fractal antenna (Fig. 29) is proposed in [162]. With an overall dimension of 60×60 mm^2, this proposed antenna achieved a huge bandwidth of 40 GHz ranging from 10 to 50 GHz. Another fractal antenna is proposed for SWB application which is made of iterations of a hexagonal slot inside a circular metallic patch to achieve a
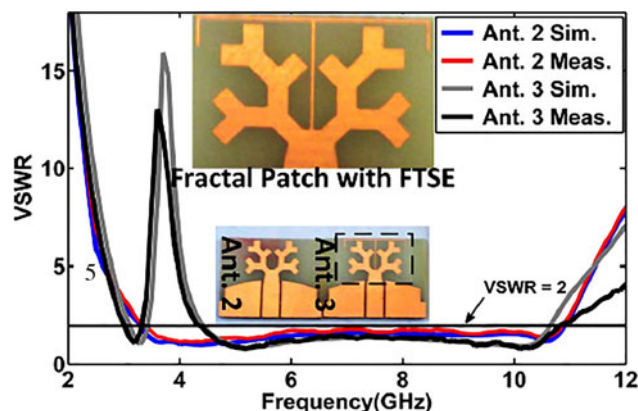

Fig. 27. (a) Fabricated prototype of different iterations of the antenna [Ant I to Ant V]. (b) Simulated and measured S_{11} characteristics of the antenna [152].

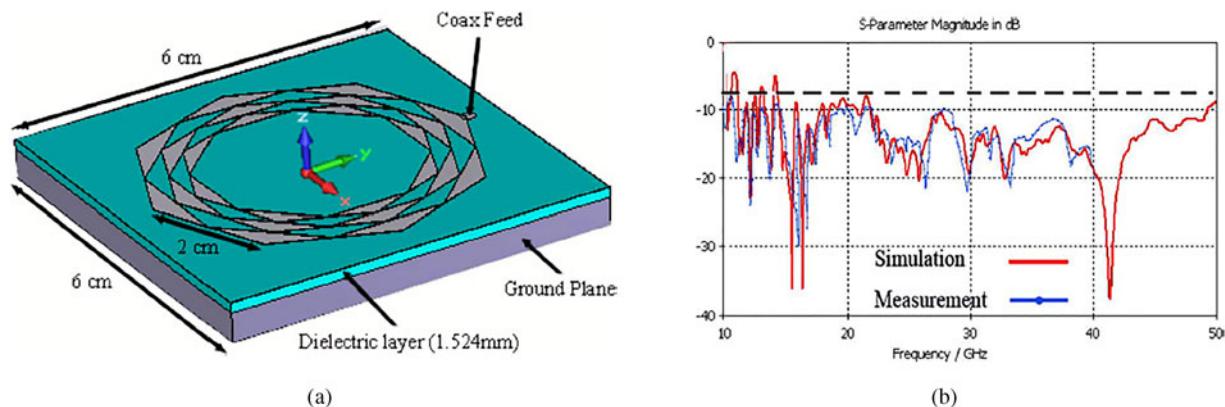Fig. 28. Simulated and measured VSWR characteristics of the antenna [158].

Fig. 29. Description of the super wideband antenna. (a) Antenna structure. (b) Simulated and measured S_{11} characteristics [162].

super-wide bandwidth ranging from 18 to 44.5 GHz [163]. A novel printed compact star-triangular fractal microstrip-fed monopole antenna with semielliptical ground plane is presented for SWB [164] applications with an operating frequency of 1–30 GHz. Based on second iteration fractal geometry and dielectric resonator, a compact SWB antenna [165] has been simulated and experimentally tested where the results from both approaches are found in good agreement. This proposed design (Fig. 30) is a super-wideband antenna that is applicable for frequencies between 2 and 40 GHz where both the radiation efficiency and the gain are acceptable for antenna applications.

In [166], a log-periodic square fractal geometry is presented for the design of a miniaturized patch antenna for the UWB applications where a miniaturization factor of 23% is achieved with a constant and stable gain in the desired band. A dongle sized quasi self-complementary UWB antenna is presented in [167]. The antenna has a hexagonal-shaped boundary with first iteration Von Koch fractal shape which is embedded on it to improve the impedance matching at higher frequencies. It has a capability to radiate at Bluetooth frequency band with additional band notch characteristics at WLAN frequency. In [168], a super-wideband Koch snowflake fractal monopole slot antenna for different wireless/multiband applications is presented. It comprises of a modified star-shaped patch where self-similarity and space-

filling features of Koch iteration technique have been employed to achieve the antenna compactness and broadband performances. In [169], a combination of triangular Koch, square Koch, tree, and Giuseppe Peano fractals are applied to the branches of log-periodic dipole microstrip antennas to generate end-fire radiation characteristics for ultrawideband applications. In [170], a new design of a compact fractal-based UWB monopole antenna is presented which covers an ultra-wide bandwidth from 3.1 to 11 GHz (112%) along with triple-band, triple-sense circular polarization (CP).

Based on a compact quad-circular monopole (Fig. 31), this antenna consists of a combination of fractal parasitic ring resonator, a triangular ring resonator, rectangular ring resonator, and modified "T"- and "I"-shaped slots on the ground plane along with a rectangular stub with "E"-shaped slot on the right side of the monopole. The proposed antenna is able to radiate left-hand circularly polarized wave at lower and mid-frequency bands, and also capable of radiating right-hand circularly polarized wave at upper frequency band. A novel fractal-evolved modified hexagonal Sierpinski grid carpet dipole has been presented in [171] which has a size of about 1.5λ in upper frequency band. With self-similarity and periodicity of fractal geometry, it maintains UWB bandwidth along with high gain, due to a so-called "array effect of element antenna". In [172], the work presents a
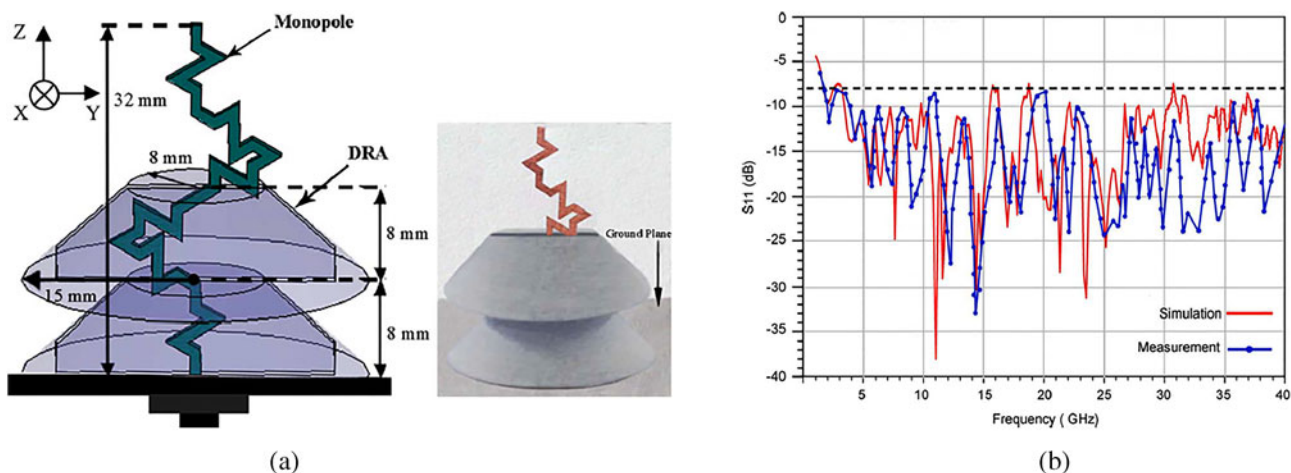

Fig. 30. Description of the antenna characteristics. (a) Antenna structure. (b) Simulated and measured S_{11} characteristics [165].
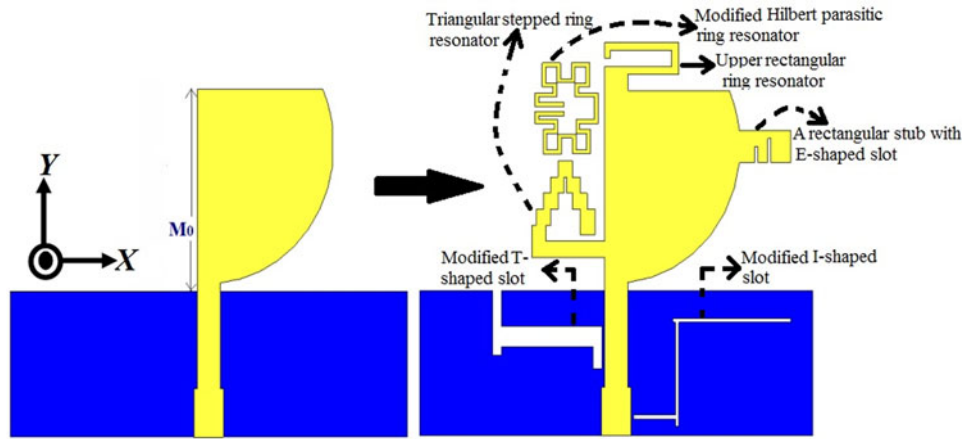
Fig. 31. Evolution of the proposed antenna from a basic monopole antenna (M0 = 13.5 mm) [170]. *P* = 1 *P* = 2 *P* = 3.

novel compact half split fractal annular ring DRA where three separate DRA geometries have been designed followed by comparison of its performance with conventional cylindrical dielectric resonator antenna (CDRA). The parametric studies are carried out for Koch snowflake on the CDRA. It is seen that second iteration of the fractal geometry offers better performance with a bandwidth of 57.5% with a gain of 6.56 dBi and also the fractal ring offers a wide impedance bandwidth of 74.23% with a gain of 7.6 dBi. As a whole, fractal UWB antenna design paradigm is still in its infancy and in future innovative designs may be explored in this domain.

Fractal array antennas

Several fractal geometries have been explored in the context of both antenna elements as well as spatial distribution of functions for elements in antenna arrays [4]. It is seen that the performance of an antenna array can be significantly improved using fractal techniques. Usage of fractal antenna array improves multi-beam, multi-band characteristics owing to the recursive nature of fractal which exhibit better array factor properties. The concept of fractal was first introduced in antenna array by Kim and Jaggard [173] in 1986 who developed a design methodology for quasi random arrays that is based on random fractals. Jaggard and Spielman in [174] presented electromagnetic wave interactions with a triadic Cantor target. A non-uniform linear array, known as Weierstrass array is introduced [175] and later, a synthesis method for the same is reported in [176]. Also synthesis of fractal patterns from concentric ring arrays is reported by Liang *et al.* in [177]. A novel approach to the design of frequency-independent array has been presented in [178] which is focused on describing a technique to design low side-lobe and multiband arrays. Generally fractal arrays can be formed in recursive manner through the repetitive application of a generating sub array, in which larger arrays at higher levels (i.e. *P* > 1) can be recursively constructed by a small array at stage-1 (*P* = 1). In many cases, the generating sub array has elements that are turned on and off in a certain pattern. A set of formula for copying, scaling, and translating of the generating array is then followed in order to produce a family of higher order arrays. Fast recursive algorithms for calculating the radiation patterns of fractal arrays have been extensively documented in [179]. The array factor for such self-similar fractal arrays may be expressed in the general form as:

$$AF_P(\Psi) = \prod_{p=1}^{P} GA(\delta^{p-1}\Psi), \tag{4}$$

where *GA* (*ψ*) is a scaling or expansion factor that represents the array factor associated with the generating array. The expression given in (4) has been found useful for the development of fast algorithms to calculate radiation patterns resulting from fractal arrays. Figure 32 shows the geometry for the first three stages of growth of an SC array.

The generating sub array (*P* = 1) in this case has uniformly excited (where all elements are on) and uniformly spaced (uniform spacing of *d* = *λ*/2) 3 × 3 planar array of isotropic sources, with the center element turned off or removed. The array factor for this generating array may be expressed in the normalized form as [179]

$$GA(\psi_x, \psi_y) = \frac{1}{4}[\cos(\psi_x) + \cos(\psi_y) + 2\cos(\psi_x)\cos(\psi_y)], \tag{5}$$

where,

$$\psi_x = \pi[\sin\theta\cos\phi - \sin\theta_0\cos\varphi_0] \tag{6}$$

$$\psi_y = \pi[\sin\theta\sin\phi - \sin\theta_0\sin\varphi_0], \tag{7}$$
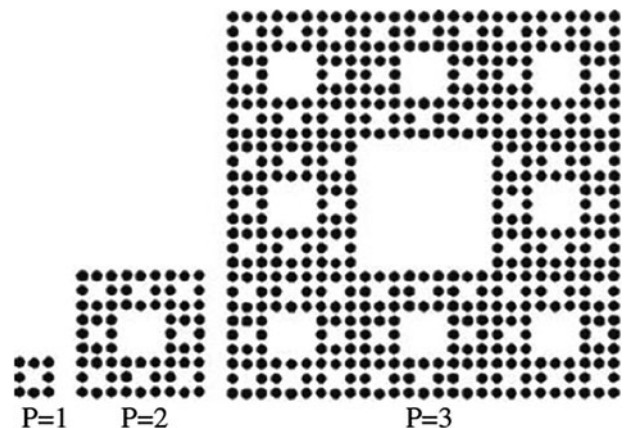

Fig. 32. Illustration of the growth of different stages of Sierpinski carpet array [179].
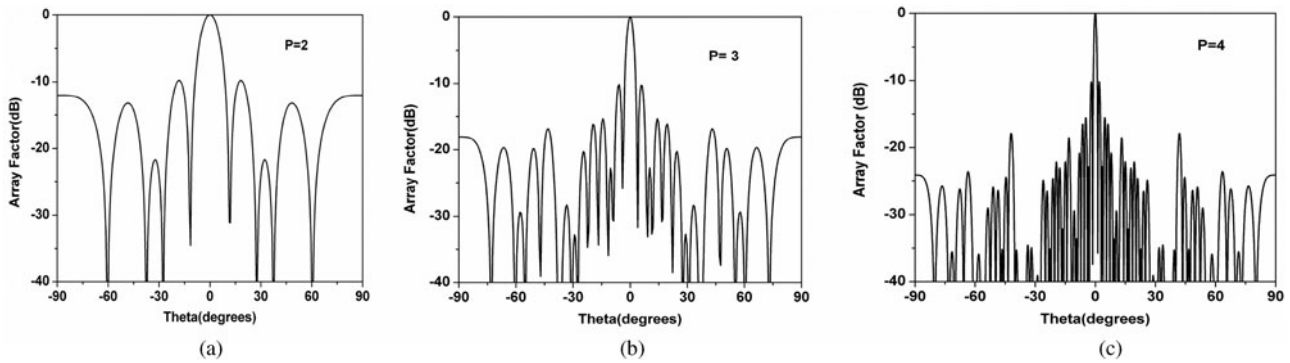
Fig. 33. Normalized far-field radiation patterns for (a) stage-2, (b) stage-3, and (c) stage-4 Sierpinski carpet fractal array using array factor expression as in (3) [180].

here, θ_0 and φ_0 represent the main beam steering angles. Choosing an expansion factor of $\delta = 3$ leads to the following expression for SC array factor for stage P.

$$AF_p(\psi_x, \psi_y) = \frac{1}{4^p} \prod_{p=1}^{P} [\cos(3^{p-1}\psi_x) + \cos(3^{p-1}\psi_y) \\ + 2\cos(3^{p-1}\psi_x)\cos(3^{p-1}\psi_y)]. \tag{8}$$

Here the element count for each recursive stage of growth P is $N_P = 8^P$ and in fact the arrays become significantly large at higher order stages. Using the above array factor expression, normalized array factor plots for various stages of the SC array are shown in Fig. 33. Due to the nature of the fractal algorithm, the array factor at n^{th} stage is produced by the multiplication of all the factors of previous stages with the array factor of the nth stage. This procedure sucessfully leads to the rapid growth of array size as well as the population of elements along with quick increment of the gain. It is seen that, due to the nature of exhibition of fractal shape, the array factor at n^{th} stage is produced by the multiplication of all the factors of previous stages with the array factor of the nth stage [179].

The array factor of conventional SC array has been considered [179] with uniform interelement spacing of $\lambda/2$ and uniform amplitude excitations for the elements which are on. This limitation puts a barrier to this fractal array factor from the application of evolutionary techniques. Also the grating lobe maxima that inevitably occurs from the gradual increase of inter-element spacing of the array elements during the process of fractal development, should be suppressed and side by side the complexity of array factor calculations in at higher stages should be simplified.

In [180], an enhancement of theoritical foundations of fractal arrays like SC is presented. This optimization is based on SCF array, where the proposed iterative matrix will reduce the usual complexity [179] for calculating the array factor of SC array at different stages of growth and also make the array factor suitable for the application of any evolutionary optimization techniques.

For planar fractal-tree arrays, a 2-D cellular automata is used in [181]. Different properties of atomic fractal arrays like multiband behavior, low side lobe level, thinning are reported in [182]. Miniaturization of wire and patch antennas using fractals has been shown in [183]. It is shown that, fractal patch array antenna significantly reduces mutual coupling between antenna elements. It is also shown that fractal designs can increase the input impedance of a small loop. The input resistance of a circular loop with a perimeter of $0.26\,\lambda$ is $1.17\,\Omega$ rather after the fourth iteration of Koch island curve with a perimeter of $0.68\,\lambda$, the structure has an input resistance of $26.7\,\Omega$ (Fig. 34).

In [184], two popular methods are presented for efficient modeling of fractal antenna array structures. A new methodology has been introduced in [185] for exploiting the self-similarity as well as the symmetry of fractal-based arrays for the development of fast algorithms toward the calculation of impedance matrix and driving point impedance. Werner et al. introduced a fractile array in [186] as a class of deterministic arrays that exhibit no grating lobes even when the spacing between the array elements is one wavelength. Some rare examples of such arrays are Peano–Gosper, terdragon, 6-terdragon, and fudge flake arrays. As an example, six-stage tetrahedron fractile array and the array factor plot are shown in Fig. 35.

It is found that neural networks [187] are an alternate approach in order to avoid the computational complexities of reconfigurable antennas. A new type of fractal-based design process has been presented that applies a robust genetic algorithm technique to evolve optimal array layouts based on polyfractal geometries [188]. Polyfractal arrays (Fig. 36) are a subset of fractal-random arrays that perform similarly; however, they are more responsive to large-scale genetic algorithm optimization.

Optimization benefit from polyfractal array geometries can be obtained because these arrays can be described by fewer
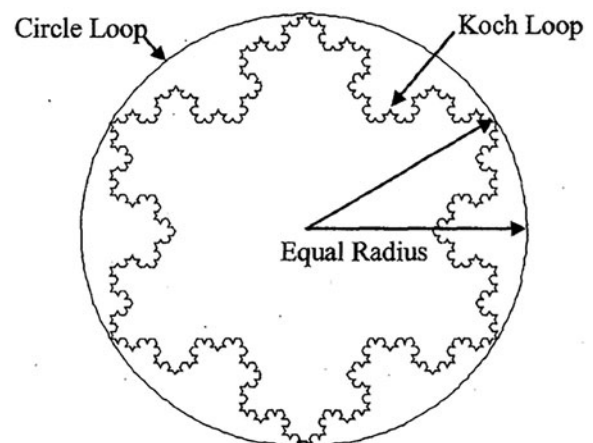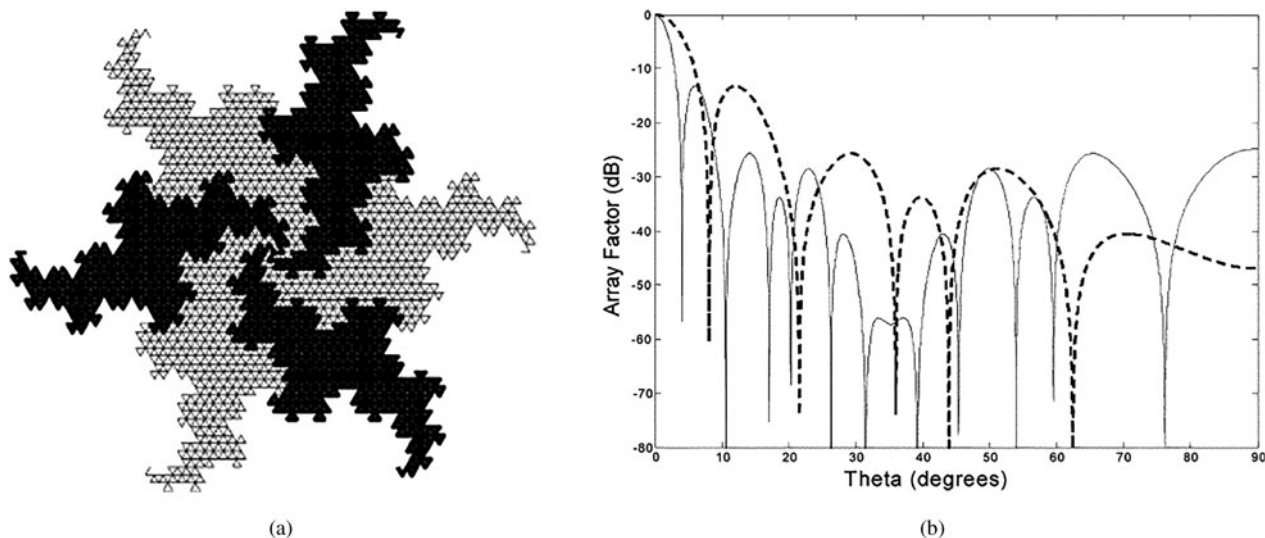

Fig. 34. Loop antenna [183].

Fig. 35. (a) Sixth stage tetrahedron fractile array. (b) Corresponding array factor plot [186].

parameters than fractal-random arrays as well as possess recursive properties which can be used for rapid beam forming algorithms. Also, the unique structure of polyfractal arrays lends itself to more general variations of the crossover and mutation operators used in the optimization of genetic algorithm. One of these specialized mutation operators, called generator autopolyploidization, can be used to stimulate the evolution process when the optimization stagnates and appears to reach premature convergence. This offers polyfractal-based genetic algorithms an efficient path to complex design solutions, by first optimizing simple designs very quickly and then adding the increasing levels of complexity only when they are finally needed. For a given number of radiating elements and beam width in the broadside direction, Cantor-based ring-thinned arrays [189] are presented (Fig. 37) for lower peak side-lobe level than one of the classical ring arrays composed of concentric rings with equal spacing between the rings. Moreover, in terms of beam width and peak side-lobe level, Cantor spiral arrays present the same performances than Cantor-based ring arrays

with the alignment of radiating elements, but with a significant reduction of 10% in the number of elements.

In [190], a new microstrip patch antenna array is proposed with fractal patches instead of conventional rectangular patches in fractal configuration. It is seen that the mutual coupling between the antenna elements decreases substantially and also the input return loss decreases compared to the rectangular patch array. Another work presented in [191] expands on poly-fractal array design methodologies by applying a robust Pareto optimization technique with the goal of reducing the peak side lobe levels at several frequencies specified over a wide operating bandwidth. A recursive beam forming algorithm and an autopolyploidy-based mutation native to polyfractal geometries are used to dramatically accelerate the genetic algorithm optimization process. This work also demonstrates that the properties of polyfractal arrays can be exploited to create designs with minimized grating lobes and relatively low side lobe levels over ultrawide bandwidths. A switched-beam antenna
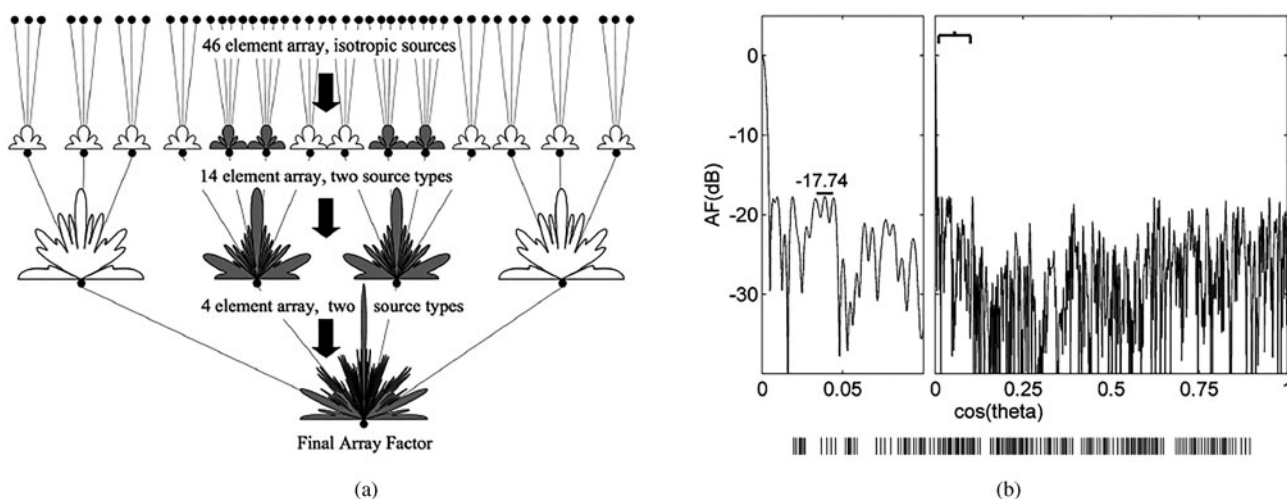

Fig. 36. (a) Illustration of the rapid recursive beam forming algorithm for a two generator polyfractal array. (b) Radiation pattern and element layout of a 178-element genetically optimized polyfractal array [188].
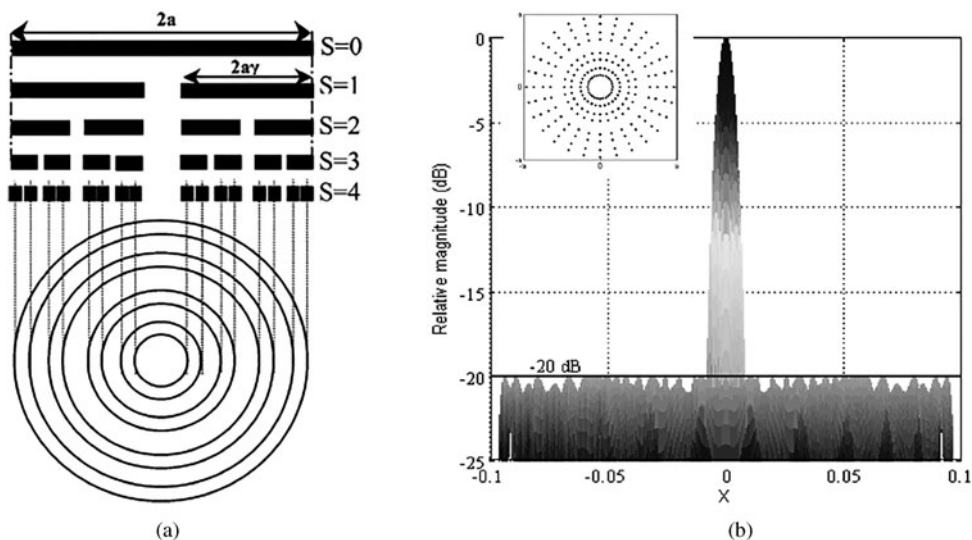
Fig. 37. (a) Symmetric Polyadic Cantor set at stage of growth at S = 1,2,3,4 and resulting concentric ring at stage 4. (b) Normalized array factor of the cantor-based ring array ($N = 1$, $\gamma = 0.4367$, $a = 56.23\lambda$, and $S = 4$) [189].

with reduced size and broadside beam based on the fractal Butler feeding network and fractal patch antenna array is presented in [192]. The circuit sizes of the fractal-shaped branch-line couplers, 0 dB crossovers, and patch antennas are 43.7, 50.1, and 74% smaller than their conventional counterparts, respectively. A four-beam prototype has been constructed. Measurement indicates that broadside beams with side lobes below −10 dB are achieved. In [193], a novel nature-inspired design process has been proposed with specially formulated genetic algorithm technique to evolve optimal polyfractal array geometries. Customized routines for the genetic algorithm have been introduced that embody and utilize the unique geometry of the polyfractal array. In addition, the self-similar characteristics of the polyfractal array have been exploited to create a recursive beam forming algorithm, making faster array factor calculations which dramatically reduces the time required for the genetic algorithm to converge. Based on perturbed Peano–Gosper array geometries, an effective design technique for generating modular, wideband phased arrays (Fig. 38) has been introduced in [194].

Unlike conventional perturbation techniques with independent adjustment of position of every element in an array, this technique is based on perturbing only six element locations along a

Fig. 38. (a) Example of a stage-1 generating array with perturbed element locations. The solid line denotes the PG curve and the dashed line denotes the initiator curve. (b) Stage-2 and (c) stage-3 arrays. (d) Geometry of a stage-3 Peano–Gosper array and with a contour plot of its normalized radiation pattern [194].

stage-1 Peano–Gosper generator curve and then using these locations to iteratively construct larger arrays which allows for a tractable perturbation process that is easily combined with any optimization techniques. Hybri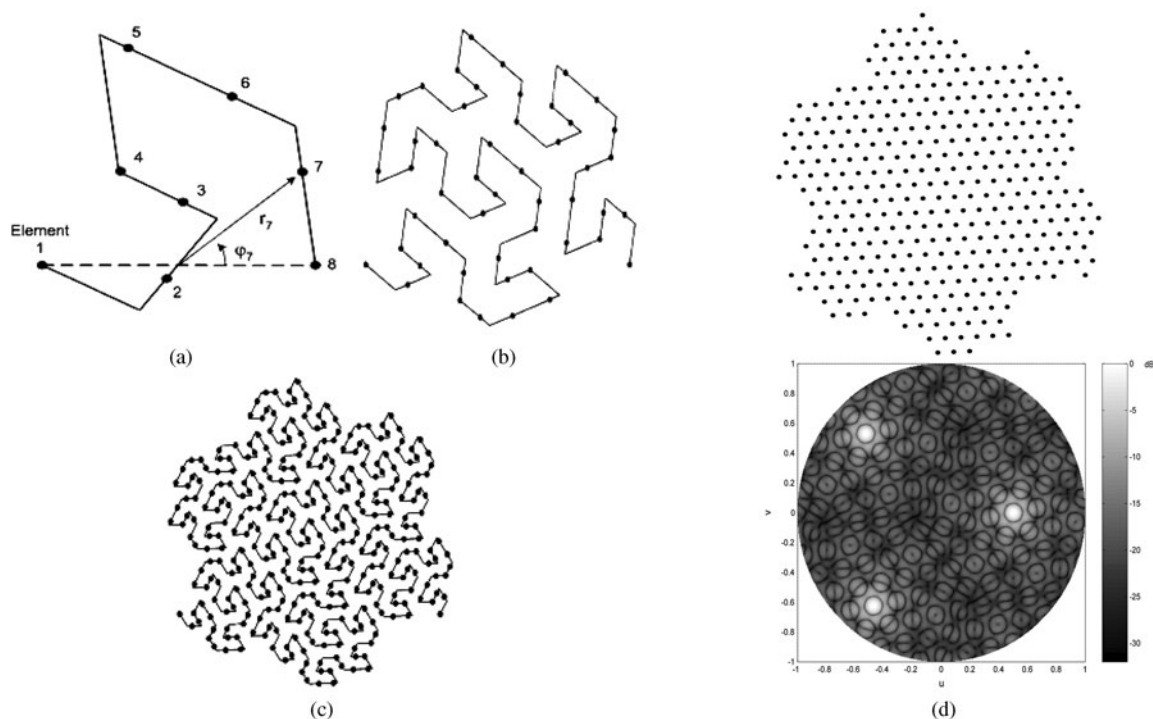d fractal direct radiating arrays with high-performance features and suitable for satellite applications are synthesized in [195]. The main advantage of the proposed arrays is the very small number of elements and driving points which leads to a feeding network of low-cost and complexity. It has been shown that nature-inspired array design methodologies can provide solutions that exhibit these ultra-wideband characteristics. In [196], the article provides an overview of two such designs: linear polyfractal arrays and planar arrays of aperiodic tilting's. Robust nature-inspired genetic-algorithm optimization techniques were utilized in this design of both types of arrays in order to achieve the best-possible UWB performance. It is shown that arrays based on Gosper curves possess several attractive properties including broadband capabilities, low sidelobes, uniform amplitude excitations, the ability to use recursive pattern formulations, and modular sub array architectures. They also offer a range of array sizes and modular configurations that are not inherent to conventional Peano–Gosper arrays. It is seen that generalized Gosper space-filling curves [197] can be suitabel to a variety of electromagnetics and antenna applications. Arrays based on these curves possess several attractive properties which include broadband capabilities, low sidelobes, uniform amplitude excitations, the ability to use recursive pattern formulations as well as modular sub-array architectures and also offers modular configurations which are not inherent to conventional Peano–Gosper arrays.

A novel multi-band antenna [198] is designed and manufactured by combining a fractal shape and DGS achieving superior performances yet within a compact architecture which makes this design suitable for geostationary satellite communications (Fig. 39). In this structure, Apollonius circles are utilized in order to design a sui generis fractal shape which was etched on the ground face of the antenna to tune different frequency bands. Finally, the designed antenna elements are aligned to build 2×2 array antenna structure. In [199], a new antenna array is designed to to combine multi-band [200] features of thinned fractal antenna arrays with the adaptive beam forming requirements. In [201], a decoupling metamaterial (MTM) configuration based on fractal EMBG structure is presented to enhance the isolation between transmitting and receiving antenna elements in a closely packed patch antenna array.

This section focused on the design aspects of fractal arrays and the optimization techniques which are one of the key tools for the enchantment of fractal antenna array behavior. In this manner, various optimization techniques have been applied by various researchers to improve array factor properties as well as to reduce the antenna elements at larger iteration levels. Still there is good scope to do a wider research work in this combination.

Conclusion

Fractal geometry has many applications in life and opened up innovative research directions in almost all branches of science and engineering gaining from the new insights it has provided. The primary focus of this review article is to summarize the developments in the field of fractal antenna engineering with basic discussions and examples. It is not possible to cite every published work on fractals still It has covered more than 200 articles that provides basic performance properties of various types of fractal antennas and arrays which has a wide range of applications. The review article reveals that fractal loop and dipole wire radiators are contrasted with linear loop and dipole antennas leading to miniaturization. When revisiting wideband antennas based on fractal, it is seen that in comparison to Euclidian UWB antennas, fractal UWB antennas possess not only small size, light weight, and thin shape for portable devices that have a rigorous limitation of space, but also wide bandwidth and good radiation characteristics with lower cross polar level. It is also seen that the concept of fractal can be applied to the design and analysis of arrays by either analyzing the array using fractal theory or by placing elements in fractal arrangement. Needless to say that the ideas of fractal geometry have been in existence for a long time but the emerging interest in fractal antennas has essentially ridden on the back of advances in computer development. In last word, the author apologize to researcher community if any novel contribution in this domain is skipped unknowingly and unintentionaly during this review process.

References

1. **Mandelbrot BB** (1983) *The Fractal Geometry of Nature*. San Francisco, CA: Freeman.
2. **Peitgen HO, Jurgens H and Saupe D** (1992) *Chaos and Fractals: New Frontiers of Science*. New York: Springer Verlag, Inc.
3. **Werner DH and Mittra R** (2000) *Frontiers in Electromagnetics*. New York: Wiley-IEEE Press.
4. **Werner DH and Ganguly S** (2003) An overview of fractal antenna engineering research. *IEEE Antennas and Propagation Magazine* **45**, 38–57.
5. **Werner DH** (1994) Fractal radiators. *Proceedings of the 4th Annual 1994 IEEE Mohawk Valley Section Dual-Use Technologies and Applications Conference*, vol. I, SUNY Institute of Technology at Utica/ Rome, New York, May 23–26, pp. 478–482.
6. **Cohen N** (1995) Fractal antennas: part 1. *Communications Quarterly*, summer, 7–22.
7. **Cohen N and Hohlfeld RG** (1996) Fractal loops and the small loop approximation. *Communications Quarterly*, Winter, pp. 77–81.
8. **Cohen N** (1996) Fractal and shaped dipoles. *Communications Quarterly*, Spring, 25–36.
9. **Cohen N** (1996) Fractal antennas: part 2. *Communications Quarterly*, Summer, 53–66.
10. **Cohen N** (1997) NEC2 modelling of fractal element antennas (FES's). *13th Annual Review of the Progress in Applied Computational*
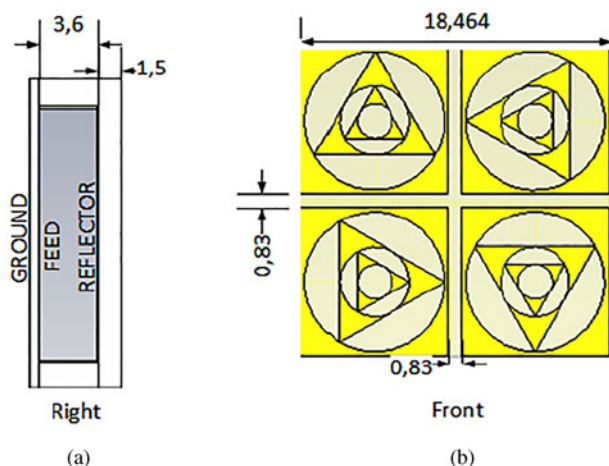
Fig. 39. Antenna array dimension. (a) Side view. (b) Front view [Dimensions are in 'mm'] [198].

Electromagnetics (ACES), vol.1, Naval Postgraduate School, Monterey, CA, pp. 297–304.

11. **Cohen N** (1997) Fractal antenna applications in wireless telecommunications. *Proceedings of the Electronics Industries Forum of New England*, pp. 43–49.

12. **Puente C, Romeu J, Pous R, Ramis J and Hijazo A** (1998) Small but long Koch fractal Monopole. *Electronics Letters* **34**, 9–10.

13. **Puente C, Romeu J and Cardama A** (2000) The Koch monopole: a small fractal antenna. *IEEE Transactions on Antennas and Propagation* **48**, 1773–1781.

14. **Petko JS and Werner DH** (2004) Miniature reconfigurable three-dimensional fractal tree antennas. *IEEE Transactions on Antennas and Propagation* **52**, 1945–1956.

15. **Rmili H, Mrabet OE, Floc'h JM and Miane JL** (2007) Study of an electrochemically-deposited 3-D random fractal tree-monopole antenna. *IEEE Transactions on Antennas and Propagation* **55**, 1045–1050.

16. **Karami A and Karami E** (2003) Fractal wired loop triangle antenna. *IEEE ICECS*, 1216–1219.

17. **Zainud-Deen SH, Awadalla KH, Khamis SH and El_shalaby NA** (2004) Radiation and scattering from Koch fractal antenna. (*URSI*) 21st *National Radio Science Conference* (*NRSC*-2004), (NTI) March 16–18, 2004, B$_8$ (1–9).

18. **Puente C, Romeu J, Pous R, Garcia X and Benítez F** (1996) Fractal multiband antenna based on the Sierpinski gasket. *Electronics Letters* **32**, 1–2.

19. **Romeu J and Soler J** (2001) Generalized Sierpinski fractal multiband antenna. *IEEE Transactions on Antennas and Propagation* **49**, 1237–1239.

20. **Best SR** (2002) On the significance of self similar fractal geometry in determining the multiband behaviour of the Sierpinski gasket antenna. *IEEE Antennas and Wireless Propagation Letters* **1**, 22–25.

21. **Best SR** (2002) Operating band comparison of the perturbed Sierpinski and modified Parany gasket antennas. *IEEE Antennas and Wireless Propagation Letters* **1**, 35–38.

22. **Mishra RK, Ghatak R and Poddar DR** (2008) Design formula for Sierpinski gasket pre-fractal planar-monopole antennas. *IEEE Antennas and Propagation Magazine* **50**, 104–107.

23. **Song CTP, Hall PS, Ghafouri- Shiraz H and Wake D** (1999) Sierpinski monopole antenna with controlled band spacing and input impedance. *Electronics Letters* **35**, 1036–1037.

24. **Song CTP, Hall PS and Ghafouri-Shiraz H** (2003) Multiband multiple ring monopole antennas. *IEEE Transactions on Antennas and Propagation* **51**, 724–729.

25. **Song CTP, Hall PS and Ghafouri-Shiraz H** (2003) Perturbed Sierpinski multiband fractal antenna with improved feeding technique. *IEEE Transactions on Antennas and Propagation* **51**, 1011–1017.

26. **Anguera J, Martandiacute E, Puente C, Borja C and Soler J** (2006) Broad-band triple-frequency microstrip patch radiator combining a dual-band modified Sierpinski fractal and a monoband antenna. *IEEE Transactions on Antennas and Propagation* **54**, 3367–3373.

27. **Hwang KC** (2007) A modified Sierpinski fractal antenna for multiband application. *IEEE Antennas Wireless Propagation Letter* **6**, 357–360.

28. **Kingsley N, Anagnostou DE, Tentzeris M and Papapolymerou J** (2007) RF MEMS sequentially reconfigurable Sierpinski antenna on a flexible organic substrate with novel DC-biasing technique. *Journal of Microelectromechanical Systems* **16**, 1185–1192.

29. **Hwang KC** (2009) Dual-wideband monopole antenna using a modified half-Sierpinski fractal gasket. *Electronics Letters* **45**, 487–489.

30. **Tsachtsiris GF, Soras CF, Karaboikis MP and Makios VT** (2004) Analysis of a modified Sierpinski gasket monopole antenna printed on dual band wireless devices. *IEEE Transactions on Antennas and Propagation* **52**, 2571–2579.

31. **Krzysztofik WJ** (2009) Modified Sierpinski fractal monopole for ISM-bands handset applications. *IEEE Transactions on Antennas and Propagation* **57**, 606–615.

32. **Soh PJ, Vandenbosch GAE, Ooi SL and Husna MRN** (2011) Wearable dual-band Sierpinski fractal PIFA using conductive fabric. *Electronics Letters* **47**, 365–367.

33. **Marnat L, Carreno AA and Conchouso D** (2013) New movable plate for efficient millimeter wave vertical on-chip antenna. *IEEE Transactions on Antennas and Propagation* **61**, 1608–1615.

34. **Walker GJ and James JR** (1998) Fractal volume antennas. *Electronics Letters* **34**, 1536–1537.

35. **Rahim MKA, Abdullah N and Aziz M** (2005) Microstrip Sierpinski carpet antenna design. *Proceedings of Asia Pacific Conf. on Applied Electromagnetics*, pp. 58–61.

36. **Ghatak R, Mishra RK and Poddar DR** (2008) Perturbed Sierpinski carpet antenna with CPW feed for IEEE 802. 11 a/b WLAN application. *IEEE Antennas and Wireless Propagation Letters* **7**, 742–744.

37. **Li H, Khan S, Liu J and He S** (2009) Parametric analysis of Sierpinski-like fractal patch antenna for compact and dual band WLAN applications. *Microwave and Optical Technology Letters* **51**, 36–40.

38. **Saidatul NA, Azremi AAH, Ahmad RB, Soh PJ and Malek F** (2009) Multiband fractal planar inverted F antenna (F-PIFA) for mobile phone application. *Progress In Electromagnetics Research B* **14**, 127–148.

39. **Ooi PC and Selvan KT** (2011) A simple printed dipole antenna with dual-band behavior. *Microwave and Optical Technology Letters* **53**, 1952–1955.

40. **Guterman J, Moreira AA and Peixeiro C** (2004) Microstrip fractal antennas for multistandard terminals. *IEEE Antennas and Wireless Propagation Letters* **3**, 351–354.

41. **Anguera J, Puente C, Borja C and Soler J** (2007) Dual frequency broad-band stacked microstrip antenna using a reactive loading and a fractal-shaped radiating edge. *IEEE Antennas and Wireless Propagation Letters* **6**, 309–312.

42. **Krishna DD, Gopikrishna M, Anandan CK, Mohanan P and Vasudevan K** (2008) CPW-fed Koch fractal slot antenna for WLAN/WiMAX applications. *IEEE Antennas and Wireless Propagation Letters* **7**, 389–392.

43. **Ghatak R, Poddar DR and Mishra RK** (2009) A moment method characterization of V-Koch fractal dipole antennas. *AEU – International Journal of Electronics and Communications* **63**, 279–286.

44. **Fazal D, Khan QU and Ihsan MB** (2012) Use of partial Koch boundaries for improved return loss, gain and side lobe levels of triangular patch antenna. *Electronics Letters* **48**, 902–903.

45. **Li D and Mao JF** (2012) A Koch-like sided fractal bow-tie dipole antenna. *EEE Transactions on Antennas and Propagation* **60**, 2242–2251.

46. **Zhou J, Luo Y, You B and Yan XJ** (2012) Novel tri-band antenna end-loaded with Koch fractal loops. *Microwave and Optical Technology Letters* **54**, 620–623.

47. **Jalil MEB, Abd Rahim MK, Samsuri NA, Murad NA, Majid HA, Kamardin K and Azfar Abdullah M** (2013) Fractal Koch multiband textile antenna performance with bending, wet conditions and on the human body. *Progress In Electromagnetics Research* **140**, 633–652.

48. **Sayem AM and Ali M** (2006) Characteristics of a microstrip-FED miniature printed Hilbert slot antenna. *Progress In Electromagnetics Research* **56**, 1–18.

49. **Chang D-C, Zeng B-H and Liu J-C** (2008) CPW-fed circular fractal slot antenna design for dual-band applications. *IEEE Transactions on Antennas and Propagation* **56**, 3630–3636.

50. **Kim HB and Hwang KC** (2012) Dual-port Spidron fractal slot antenna for multiband gap-filler applications. *IEEE Transactions on Antennas and Propagation* **60**, 4940–4943.

51. **Tang PW and Wahid PF** (2004) Hexagonal fractal multiband antenna. *IEEE Antennas and Wireless Propagation Letters* **3**, 111–112.

52. **Dehkhoda P and Tavakoli A** (2004) A crown square microstrip fractal antenna. *IEEE Antennas and Propagation Society International Symposium*, 2396–2399.

53. **Azaro R, Natale FD, Donelli M, Zeni E and Massa A** (2006) Synthesis of a prefractal dual-band monopolar antenna for GPS applications. *IEEE Antennas and Wireless Propagation Letters* **5**, 361–364.

54. **Liu JC, Wu CY, Chen CH, Chang DC and Chen JY** (2006) Modified Sierpinski fractal monopole antenna with Descartes circle theorem. *Microwave and Optical Technology Letters* **48**, 909–911.

55. **Liu JC, Wu CY, Chang DC and Liu CY** (2006) Relationship between Sierpinski gasket and Apollonian packing monopole antennas. *Electronics Letters* **42**, 847–848.

56. **Azaro R, Zeni E, Rocca P and Massa A** (2007) Synthesis of a Galileo and Wi-max three-band. *IEEE Antennas and Wireless Propagation Letters* 6, 510–514.

57. **Sinha SN and Jain M** (2007) A self-affine fractal multiband antenna. *IEEE Antennas and Wireless Propagation Letters* 6, 110–112.

58. **Lee YC and Sun JS** (2008) A fractal dipole tag antenna for RFID dual-band application. *Microwave and Optical Technology Letters* 50, 1963–1966.

59. **Manimegalai B, Raju S and Abhaikumar V** (2009) A multifractal cantor antenna for multiband wireless applications. *IEEE Antennas and Wireless Propagation Letters* 8, 359–362.

60. **Ghosh B, Sinha SN and Kartikeyan MV** (2009) Radiation from cavity-backed fractal aperture antennas. *Progress In Electromagnetics Research C* 11, 155–170.

61. **Gemio J, Granados J and Castany J** (2009) Dual-band antenna with fractal-based ground plane for WLAN applications. *IEEE Antennas and Wireless Propagation Letters* 8, 748–751.

62. **Ghatak R, Poddar DR and Mishra RK** (2009) Design of Sierpinski gasket fractal microstrip antenna using real coded genetic algorithm. *IET Microwaves Antennas and Propagation* 3, 1133–1140.

63. **Azaro R, Viani F, Lizzi L, Zeni E and Massa A** (2009) A monopolar quad-band antenna based on a Hilbert self-affine pre-fractal geometry. *IEEE Antennas and Wireless Propagation Letters* 8, 177–180.

64. **Bor SS, Lu TC, Liu JC and Zeng BH** (2009) Fractal monopole-like antenna with series Hilbert-curves for WLAN dual-band and circular polarization applications. *Microwave and Optical Technology Letters* 51, 876–880.

65. **Azaro R, Debiasi L, Zeni E, Benedetti M, Rocca P and Massa A** (2009) A hybrid prefractal three-band antenna for multistandard mobile wireless applications. *IEEE Antennas and Wireless Propagation Letters* 8, 905–908.

66. **Rmili H, Floch J and Zangar H** (2009) Experimental study of a 2-D irregular fractal-jet printed antenna. *IEEE Antennas and Wireless Propagation Letters* 8, 328–331.

67. **Mahatthanajatuphat C, Saleekaw S and Akkaraekthalin P** (2009) A Rhombic patch monopole antenna with modified Minkowski fractal geometry for UMTS, WLAN, and mobile WiMAX application. *Progress In Electromagnetics Research* 89, 57–74.

68. **Kimouche H, Zemmour H and Atrouz B** (2009) Dual-band fractal shape antenna design for RFID applications. *Electronics Letters* 45, 1061–1063.

69. **Pourahmadazar J, Ghobadi C, Nourinia J and Shirzad H** (2010) Multiband ring fractal monopole antenna for mobile devices. *IEEE Antennas and Wireless Propagation Letters* 9, 863–866.

70. **Hong T, Gong SX, Liu Y and Jiang W** (2010) Monopole antenna with quasi-fractal slotted ground plane for dual-band applications. *IEEE Antennas and Wireless Propagation Letters* 9, 595–598.

71. **Liu JC, Zeng BH, Chen HL, Bor SS and Chang DC** (2010) Compact fractal antenna with self-complementary Hilbert curves for WLAN dual-band and circular polarization applications. *Microwave and Optical Technology Letters* 52, 2535–2539.

72. **Vinoy KJ and Pal A** (2010) Dual-frequency characteristics of Minkowski-square ring antennas. *IET Microwaves, Antennas and Propagation* 4, 219–224.

73. **Thakare YB and Kumar R** (2010) Design of fractal patch antenna for size and radar cross-section reduction. *IET Microwaves, Antennas and Propagation* 4, 175–181.

74. **Bayatmaku N, Lotfi P, Azarmanesh M and Soltani S** (2011) Design of simple multi-band patch antenna for mobile communication applications using new E-shape fractal. *IEEE Antennas and Wireless Propagation Letters* 10, 873–875.

75. **Eichler J, Hazdra P, Capek M, Korinek T and Hamouz P** (2011) Design of dual band orthogonally polarized L-probe fed fractal patch antenna using modal methods. *IEEE Antennas and Wireless Propagation Letters* 10, 1389–1392.

76. **Patnaik AA and Sinha SN** (2011) Design of custom-made fractal multi-band antennas using ANN-PSO. *IEEE Antennas and Propagation Magazine* 53, 94–101.

77. **Lizzi L and Massa A** (2011) Dual-band printed fractal monopole antenna for LTE applications. *IEEE Antennas and Wireless Propagation Letters* 10, 760–763.

78. **Chaimool S, Chokchai C and Akkaraekthalin P** (2012) Multiband loaded fractal loop monopole antenna for USB dongle applications. *Electronics Letters* 48, 1446–1447.

79. **Oraizi H and Hedayati S** (2012) Circularly polarized multiband microstrip antenna using the square and Giuseppe Peano fractals. *IEEE Transactions on Antennas and Propagation* 60, 3466–3470.

80. **Behera S and Vinoy KJ** (2012) Multi-port network approach for the analysis of dual band fractal microstrip antennas. *IEEE Transactions on Antennas and Propagation* 60, 5100–5106.

81. **Liu G, Xu L and Wu Z** (2013) Dual-band microstrip RFID antenna with tree-like fractal structure. *IEEE Antennas and Wireless Propagation Letters* 12, 976–978.

82. **Varadhan C, Pakkathillam JK, Kanagasabai M, Sivasamy R, Natarajan R and Palaniswamy SK** (2013) Triband antenna structures for RFID systems deploying fractal geometry. *IEEE Antennas and Wireless Propagation Letters* 12, 437–440.

83. **Choukiker YK, Sharma SK and Behera SK** (2014) Hybrid fractal shape planar monopole antenna covering multiband wireless communications with MIMO implementation for handheld mobile devices. *IEEE Transactions on Antennas and Propagation* 62, 1483–1488.

84. **Barroso R, Mata O and Diaz M** (2014) 4-Stage parany monopole with side triangular complements and side-notched vertices. *IEEE Antennas and Wireless Propagation Letters* 13, 1397–1400.

85. **Cai T, Wang G, Zhang X and Shi J** (2015) Low-profile compact circularly-polarized antenna based on fractal metasurface and fractal resonator. *IEEE Antennas and Wireless Propagation Letters* 14, 1072–1076.

86. **Dhar S, Patra K, Ghatak R, Gupta B and Poddar DR** (2015) A dielectric resonator-loaded Minkowski fractal-shaped slot loop heptaband antenna. *IEEE Transactions on Antennas and Propagation* 63, 1521–1529.

87. **Farswan A, Gautam AK, Kanaujia BK and Rambabu K** (2016) Design of Koch fractal circularly polarized antenna for handheld UHF RFID reader applications. *IEEE Transactions on Antennas and Propagation* 64, 771–775.

88. **Orazi H and Soleimani H** (2015) Miniaturisation of the triangular patch antenna by the novel dual-reverse-arrow fractal. *IET Microwaves, Antennas & Propagation* 9, 627–633.

89. **Ratilal Prajapati P, Gopala Krishna Murthy G, Patnaik A and Venkata Kartikeyan M** (2015) Design and testing of a compact circularly polarised microstrip antenna with fractal defected ground structure for L-band applications. *IET Microwaves, Antennas & Propagation* 9, 1179–1185.

90. **Taghadosi M, Albasha L, Qaddoumi N and Ali M** (2015) Miniaturised printed elliptical nested fractal multiband antenna for energy harvesting applications. *IET Microwaves, Antennas & Propagation* 9, 1045–1053.

91. **Velan S, Sundarsingh EF, Kanagasabai M, Sarma AK, Raviteja C, Sivasamy R and Pakkathillam JK** (2015) Dual-band EBG integrated monopole antenna deploying fractal geometry for wearable applications. *IEEE Antennas and Wireless Propagation Letters* 14, 249–252.

92. **Wang R, Wang B, Gong Z and Ding X** (2015) Compact multiport antenna with radiator-sharing approach and its performance evaluation of time reversal in an intra-car environment. *IEEE Transactions on Antennas and Propagation* 63, 4213–4219.

93. **Alibakhshi-Kenari M, Naser-Moghadasi M, Ali Sadeghzadeh R, Virdee BS and Limiti E** (2016) Dual-band RFID tag antenna based on the Hilbert-curve fractal for HF and UHF applications. *IET Circuits, Devices & Systems* 10, 140–146.

94. **Wang Y, Wang Z and Li J** (2017) UHF Moore fractal antennas for online GIS PD detection. *IEEE Antennas and Wireless Propagation Letters* 16, 852–855.

95. **Kgwadi M and Drysdale TD** (2016) Diode-switched thermal-transfer printed antenna on flexible substrate. *Electronics Letters* 52, 258–260.

96. **Jun SY, Sanz-Izquierdo B, Parker EA, Bird D and McClelland A** (2017) Manufacturing considerations in the 3-D printing of fractal antennas. *IEEE Transactions on Components, Packaging and Manufacturing Technology* 7, 1891–1898.

97. **Wei K, Li JY, Wang L, Xu R and Xing ZJ** (2017) A new technique to design circularly polarized microstrip antenna by fractal defected ground

structure. *IEEE Transactions on Antennas and Propagation* **65**, 3721–3725.

98. **Chuma EL, de la Torre Rodríguez L, Iano Y, Bravo Roger LL and Sanchez-Soriano M-A** (2018) Compact rectenna based on a fractal geometry with a high conversion energy efficiency per area. *IET Microwaves Antennas and Propagation* **12**, 173–178.

99. **Anguera J, Andújar A, Benavente S, Jayasinghe J and Kahng S** (2018) High-directivity microstrip antenna with Mandelbrot fractal boundary. *IET Microwaves, Antennas & Propagation* **12**, 569–575.

100. **Braham Chaouche Y, Messaoudene I, Benmabrouk I, Nedil M and Bouttout F** (2019) A compact CPW-fed reconfigurable fractal antenna for switchable multiband systems. *IET Microwaves, Antennas Propagation* **13**, 1–8.

101. **Goswami C, Ghatak R and Poddar DR** (2018) Multi-band bisected Hilbert monopole antenna loaded with multiple sub wavelength split-ring resonators. *IET Microwaves, Antennas & Propagation* **12**, 1719–1727.

102. **Mohammad Husain Ranjbaran S and Mohanna S** (2018) Improved spiral antenna with a new semi-fractal reflector for short-range sensing. *IET Microwaves, Antennas & Propagation* **12**, 1839–1845.

103. **Sharma V, Lakwar N, Kumar N and Garg T** (2018) Multiband low-cost fractal antenna based on parasitic split ring resonators. *IET Microwaves, Antennas & Propagation* **12**, 913–919.

104. **Abed AT, Jit Singh MS and Islam MT** (2018) Compact fractal antenna circularly polarised radiation for Wi-Fi and WiMAX communications. *IET Microwaves, Antennas & Propagation* **12**, 2218–2224.

105. **Elwi TA, Asaad Abdul Hassain Z and Almukhtar Tawfeeq O** (2019) Hilbert metamaterial printed antenna based on organic substrates for energy harvesting. *IET Microwaves, Antennas & Propagation* **13**, 2185–2192.

106. **Ghatak R, Mishra RK and Poddar DR** (2007) Stacked dual layer complementing Sierpinski gasket planar antenna. *Microwave and Optical Technology Letters* **49**, 2831–2833.

107. **Tiwari H and Kartikeyan MV** (2010) A stacked microstrip patch antenna with fractal shaped defects. *Progress In Electromagnetics Research C* **14**, 185–195.

108. **Malik J and Kartikeyan MV** (2011) A stacked equilateral triangular patch antenna with Sierpinski gasket fractal for WLAN applications. *Progress In Electromagnetics Research Letters* **22**, 71–81.

109. **Hung TF, Liu JC, Bor SS and Chen CC** (2012) Compact single-feed circularly polarized aperture-coupled stack antenna with Minkowski-island-based fractal patch. *Microwave and Optical Technology Letters* **54**, 2278–2283.

110. **Hung TF, Liu JC, Wei CY, Chen CC and Bor SS** (2014) Dual-band circularly polarized aperture-coupled stack antenna with fractal patch for WLAN and WiMAX applications. *International Journal of RF and Microwave Computer Aided Engineering* **24**, 130–138.

111. **Liu JC, Chang DC, Soong D, Chen CH, Wu CY and Yao K** (2005) Circular fractal antenna approaches with Descartes circle theorem for multiband/wideband applications. *Microwave and Optical Technology Letters* **44**, 404–408.

112. **Lee GS** (2003) A uniplanar wideband loop-antenna design using an alternate inverted 2D cantor set sequence. *Microwave and Optical Technology Letters* **39**, 437–439.

113. **Mirzapour B and Neyestanak AAL** (2007) Enhanced wideband and compact size fractal Kokh antenna. *Microwave and Optical Technology Letters* **49**, 1077–1080.

114. **Mirzapour B and Hassani HR** (2008) Size reduction and bandwidth enhancement of snowflake fractal antenna. *IET Microwaves, Antennas and Propagation* **2**, 180–187.

115. **Patnam RH** (2008) Broadband CPW-fed planar Koch fractal loop antenna. *IEEE Antennas and Wireless Propagation Letters* **7**, 429–431.

116. **Naghshvarian-Jahromi M** (2008) Novel wideband planar fractal monopole antenna. *IEEE Transactions on Antennas and Propagation* **56**, 3844–3849.

117. **Hwang KC** (2009) Broadband circularly-polarized Spidron fractal slot antenna. *Electronics Letters* **45**, 3–4.

118. **Chen WL, Wang GM and Zhang CX** (2009) Bandwidth enhancement of a microstrip-line-fed printed wide-slot antenna with a fractal-shaped slot. *IEEE Transactions on Antennas and Propagation* **57**, 2176–2179.

119. **Anguera JJ, Daniel P, Borja C, Mumbru J, Puente C, Leduc T, Sayegrih K and Van Roy P** (2010) Metalized foams for antenna design: application to fractal-shaped Sierpinski-carpet monopole. *Progress In Electromagnetics Research* **104**, 239–251.

120. **Naghshvarian Jahromi M, Falahati A and Edwards RM** (2011) Bandwidth and impedance-matching enhancement of fractal monopole antennas using compact grounded coplanar waveguide. *IEEE Transactions on Antennas and Propagation* **59**, 2480–2487.

121. **Sung YJ** (2011) Bandwidth enhancement of a wide slot using fractal-shaped Sierpinski. *IEEE Transactions on Antennas and Propagation* **59**, 3076–3079.

122. **Caramanica F** (2012) Microstrip L-band antenna based on Julia prefractal curve. *Microwave and Optical Technology Letters* **54**, 2327–2330.

123. **Ghatak R, Chatterjee S and Poddar DR** (2012) Wideband fractal shaped slot antenna for X-band application. *Electronics Letters* **48**, 198–199.

124. **Hajihashemi MR and Abiri H** (2007) Parametric study of novel types of dielectric resonator antennas based on fractal geometry. *International Journal of RF and Microwave Computer Aided Engineering* **17**, 416–424.

125. **Dhar S, Ghatak R, Gupta B and Poddar DR** (2013) A wideband Minkowski fractal dielectric resonator antenna. *IEEE Transactions on Antennas and Propagation* **61**, 2895–2903.

126. **Mukherjee B, Patel P and Mukherjee J** (2014) Hemispherical dielectric resonator antenna based on Apollonian gasket of circles – a fractal approach. *IEEE Transactions on Antennas and Propagation* **62**, 40–47.

127. **Altaf A, Yang Y, Lee K and Hwang KC** (2015) Circularly polarized Spidron fractal dielectric resonator antenna. *IEEE Antennas and Wireless Propagation Letters* **14**, 1806–1809.

128. **Liu H, Liu Y, Wei M and Gong S** (2015) Dual-broadband dielectric resonator antenna based on modified Sierpinski fractal geometry. *Electronics Letters* **51**, 806–808.

129. **Zhong Y-W, Yang G-M and Zhong L-R** (2015) Gain enhancement of bow-tie antenna using fractal wideband artificial magnetic conductor ground. *Electronics Letters* **51**, 315–317.

130. **Kizhekke Pakkathillam J and Kanagasabai M** (2015) Circularly polarized broadband antenna deploying fractal slot geometry. *IEEE Antennas and Wireless Propagation Letters* **14**, 1286–1289.

131. **Harbaji MMO, Zahed AH, Habboub SA, AlMajidi MA, Assaf MJ, El-Hag AH and Qaddoumi NN** (2017) Design of Hilbert fractal antenna for partial discharge classification in oil-paper insulated system. *IEEE Sensors Journal* **17**, 1037–1045.

132. **Kumar Choukiker Y and Kumar Behera S** (2017) Wideband frequency reconfigurable Koch snowflake fractal antenna. *IET Microwaves, Antennas & Propagation* **11**, 203–208.

133. **Kiran DV, Sankaranarayanan D and Mukherjee B** (2017) Compact embedded dual-element rectangular dielectric resonator antenna combining Sierpinski and Minkowski fractals. *IEEE Transactions on Components, Packaging and Manufacturing Technology* **7**, 786–791.

134. **Wang F, Bin F, Sun Q, Fan J and Ye H** (2017) A compact UHF antenna based on complementary fractal technique. *IEEE Access* **5**, 21118–21125.

135. **Biswas B, Ghatak R and Poddar DR** (2017) A fern fractal leaf inspired wideband antipodal Vivaldi antenna for microwave imaging system. *IEEE Transactions on Antennas and Propagation* **65**, 6126–6129.

136. **Lin X, Seet B, Joseph F and Li E** (2018) Flexible fractal electromagnetic bandgap for millimeter-wave wearable antennas. *IEEE Antennas and Wireless Propagation Letters* **17**, 1281–1285.

137. **Zhang B, Yao P and Duan J** (2018) Gain-enhanced antenna backed with the fractal artificial magnetic conductor. *IET Microwaves, Antennas & Propagation* **12**, 1457–1460.

138. **Darimireddy NK, Ramana Reddy R and Mallikarjuna Prasad A** (2018) A miniaturized hexagonal-triangular fractal antenna for wide-band applications. *IEEE Antennas & Propagation Magazine* **60**, 104–110.

139. **Karmakar A, Bhattacharjee A, Saha A and Bhawal A** (2019) Design of a fractal inspired antipodal Vivaldi antenna with enhanced radiation characteristics for wideband applications. *IET Microwaves, Antennas & Propagation* **13**, 892–897.

140. **Li X-L, Yang G-M, IEEE Senior Member and Jin Y-Q** (2019) Isolation enhancement of wideband vehicular antenna array using fractal

decoupling structure. IEEE Antennas and Wireless Propagation Letters 18, 1799–1803.

141. **Mokhtari-Koushyar F, Grubb PM, Chen MY and Chen RT** (2019) A miniaturized tree-shaped fractal antenna printed on a flexible substrate. *IEEE Antennas & Propagation Magazine* 61, 60–66.

142. **Gupta S, Kshirsagar P and Mukherjee B** (2019) A low-profile multilayer cylindrical segment fractal dielectric resonator antenna. *IEEE Antennas & Propagation Magazine* 61, 55–63.

143. **Gupta S, Kshirsagar P and Mukherjee B** (2018) Sierpinski fractal inspired inverted pyramidal DRA for wide band applications. *Electromagnetics* 36, 103–112. doi: 10.1080/02726343.2018.1436738.

144. **FCC 02-48, ET-Docket 98-153, "First Report and Order", April 2002.**

145. **Rumsey V** (1966) *Frequency Independent Antennas*. New York, NY, USA: Academic.

146. **Kim C** (2010) Ultra-wideband antenna, microwave and millimetre wave technologies modern UWB antennas and equipment, Igor Mini (Ed.), ISBN: 978-953-7619-67-1, InTech, doi: 10.5772/9015.

147. **Lui WJ, Cheng CH, Cheng Y and Zhu H** (2005) Frequency notched ultra-wideband microstrip slot antenna with fractal tuning stub. *Electronics Letters* 41, 294–296.

148. **Lui WJ, Cheng CH and Zhu HB** (2006) Compact frequency notched ultra-wideband fractal printed slot antenna. *IEEE Microwave and Wireless Component Letters* 16, 224–226.

149. **Ding M, Jin R, Geng J and Wu Q** (2007) Design of a CPW-fed ultra wideband fractal antenna. *Microwave and Optical Technology Letters* 49, 173–176.

150. **Naeem Khan S, Hu J, Xiong J and He S** (2008) Circular fractal monopole antenna based on Descartes circle theorem for UWB application. *Microwave and Optical Technology Letters* 50, 1605–1608.

151. **Oraizi H and Hedayati S** (2011) Miniaturized UWB monopole microstrip antenna design by the combination of Giuseppe Peano and Sierpinski carpet fractals. *IEEE Antennas and Wireless Propagation Letters* 10, 67–70.

152. **Pourahmadazar J, Ghobadi C and Nourinia J** (2011) Novel modified Pythagorean tree fractal monopole antennas for UWB applications. *IEEE Antennas and Wireless Propagation Letters* 10, 484–487.

153. **Jahromi MN, Falahati A and Edwards RM** (2011) Application of fractal binary tree slot to design and construct a dual band-notch CPW-ground-fed ultra-wide band antenna. *IET Microwaves Antennas and Propagation* 5, 1424–1430.

154. **Yang Y, Liu C and Jiang T** (2012) Miniaturization cantor set fractal ultra wideband antenna with a notch band characteristic. *Microwave and Optical Technology Letters* 54, 1227–1230.

155. **Fereidoony F, Chamaani S and Mirtaheri SA** (2012) Systematic design of UWB monopole antenna with stable omnidirectional radiation pattern. *IEEE Antennas and Wireless Propagation Letters* 11, 752–755.

156. **Naser-Moghadasi M, Sadeghzadeh RA, Aribi T, Sedghi T and Virdee BS** (2012) UWB Monopole microstrip antenna using fractal tree unit-cells. *Microwave and Optical Technology Letters* 54, 2366–2370.

157. **Maza AR, Cook B, Jabbour G and Shamim A** (2012) Paper-based inkjet-printed ultra-wideband fractal antennas. *IET Microwaves, Antennas and Propagation* 6, 1366–1373.

158. **Naser-Moghadasi M, Sadeghzadeh RA, Sedghi T, Aribi T and Virdee BS** (2013) UWB CPW-fed fractal patch antenna With band-notched function employing folded T-shaped element. *IEEE Antennas and Wireless Propagation Letters* 12, 504–507.

159. **Fallahi H and Atlasbaf Z** (2013) Study of a class of UWB CPW-fed monopole antenna with fractal elements. *IEEE Antennas and Wireless Propagation Letters* 12, 1484–1487.

160. **Tran D, Aubry DP, Szilagyi A, Lager IE, Yarovyi O and Ligthart LP** (2010) On the design of a super wideband antenna. In Lembrikov B (ed.), *Ultra Wideband*. InTech Publication, pp. 399–426. ISBN: 978-953-307-139-8.

161. **Lau KL, Kong KC and Luk KM** (2008) Super-wideband monopolar patch antenna. *Electronics Letters* 44, 716–718.

162. **Azari A** (2011) A new super wideband fractal microstrip antenna. *IEEE Transactions on Antennas and Propagation* 59, 1724–1727.

163. **Dorostkar MA, Islam MT and Azim R** (2013) Design of a novel super wide band circular-hexagonal fractal antenna. *Progress In Electromagnetics Research* 139, 229–245.

164. **Waladi V, Mohammadi N, Zehforoosh Y, Habashi A and Nourinia J** (2013) A novel modified star-triangular fractal (MSTF) monopole antenna for super-wideband applications. *IEEE Antennas and Wireless Propagation Letters* 12, 651–654.

165. **Azari A, Ismail A, Sali A and Hashim F** (2013) A new super wideband fractal monopole-dielectric resonator antenna. *IEEE Antennas and Wireless Propagation Letters* 12, 1014–1016.

166. **Amini A, Oraizi H and Chaychi zadeh MA** (2015) Miniaturized UWB log-periodic square fractal antenna. *IEEE Antennas and Wireless Propagation Letters* 14, 1322–1325.

167. **Gorai A, Pal M and Ghatak R** (2017) A compact fractal-shaped antenna for ultrawideband and Bluetooth wireless systems with WLAN rejection functionality. *IEEE Antennas and Wireless Propagation Letters* 16, 2163–2166.

168. **Manohar M** (2019) Miniaturised low-profile super-wideband Koch snowflake fractal monopole slot antenna with improved BW and stabilised radiation pattern. *IET Microwaves, Antennas & Propagation* 13, 1948–1954.

169. **Oraizi H, Amini A and Karimi Mehr M** (2017) Design of miniaturised UWB log-periodic end-fire antenna using several fractals with WLAN band-rejection. *IET Microwaves, Antennas & Propagation* 11, 193–202.

170. **Karmakar A, Chakraborty P, Banerjee U and Saha A** (2019) Combined triple band circularly polarised and compact UWB monopole antenna. *IET Microwaves, Antennas & Propagation* 13, 1306–1311.

171. **Li D, Wu Z and Mao J-F** (2019) Ultra-wideband high-gain dipole antenna evolved from hexagonal Sierpinski grid fractal gasket. *IET Microwaves, Antennas & Propagation* 13, 574–583.

172. **Sankaranarayanan D, Venkatakiran D and Mukherjee B** (2016) A novel compact fractal ring based cylindrical dielectric resonator antenna for ultra wideband application. *Progress In Electromagnetics Research C* 67, 71–83.

173. **Kim Y and Jaggard DL** (1986) The fractal random array. *Proceedings of IEEE* 74, 1278–1280.

174. **Jaggard DL and Spielman T** (1992) Triadic cantor target diffraction. *Microwave and Optical Technology Letters* 5, 460–466.

175. **Werner DH and Werner PL** (1992) Fractal radiation pattern synthesis. *Proceedings of the URSI National Radio Science Meeting*, Boulder, Colorado, pp. 66, January 1992.

176. **Werner DH and Werner PL** (1995) On the synthesis of fractal radiation patterns. *Radio Science* 30, 29–45.

177. **Liang X, Zhensen W and Wenbing W** (1996) Synthesis of fractal patterns from concentric ring arrays. *Electronics Letters* 32, 1940–1941.

178. **Puente-Baliardia C and Pous R** (1996) Fractal design of multiband and low side-lobe array. *IEEE Transactions on Antennas and Propagation* 44, 730–739.

179. **Werner DH, Haupt RL and Werner PL** (1999) Fractal antenna engineering: the theory and design of fractal antenna arrays. *IEEE Antennas and Propagation Magazine* 41, 37–59.

180. **Karmakar A, Ghatak R, Mishra RK and Poddar DR** (2015) Sierpinski carpet fractal-based planar array optimization based on differential evolution algorithm. *Journal of Electromagnetic Waves and Applications* 29, 247–260.

181. **Sinha AK, Srivastava GP and Mehta SD** (2002) Planar fractal tree arrays derived from cellular automata. *IEE Electronics Letters* 38, 947–948.

182. **Kravchenko VF** (2003) The theory of fractal antenna arrays. IEEE International Conference on Antenna Theory and Techniques, Ukraine, pp. 183–189, September 2003.

183. **Gianvittorio J and Rahmat–Samii Y** (2002) Fractal antennas: a novel antenna miniaturization technique and applications. *IEEE Antennas and Propagation Magazine* 44, 20–35.

184. **Zygiridis TT, Kantartzis NV, Yioultsis TV and Tsibkoukis TD** (2003) Higher order approaches of FDTD and TVFE methods for the accurate analysis of fractal antenna arrays. *IEEE Transactions on Magnetics* 39, 1230–1234.

185. **Werner DH, Baldacci D and Werner PL** (2004) An efficient recursive procedure for evaluating the impedance matrix of linear and planar arrays. *IEEE Transactions on Antennas and Propagation* **52**, 380–387.

186. **Werner DH, Kuhirun W and Werner PL** (2004) Fractile arrays: a new class of tiled arrays with fractal boundaries. *IEEE Transaction on Antennas and Propagation* **52**, 2008–2018.

187. **Patnaik A, Anagnostou D, Christodolou CG and Lyke JC** (2005) Modeling frequency reconfigurable antenna array using neural networks. *Microwave and Optical Technology Letters* **44**, 351–354.

188. **Petko JS and Werner DH** (2005) The evolution of optimal linear poly-fractal arrays using genetic algorithms. *IEEE Transactions on Antennas and Propagation* **53**, 3604–3615.

189. **Hebib S, Raveu N and Aubert H** (2006) Cantor spiral array for the design of thinned arrays. *IEEE Antennas and Wireless Propagation Letters* **5**, 104–106.

190. **Yousefzadeh N, Ghobadi C and Kamyab M** (2006) Consideration of mutual coupling in a microstrip patch array using fractal elements. *Progress In Electromagnetics Research* **66**, 41–49.

191. **Petko JS and Werner DH** (2008) The pareto optimization of ultrawide-band polyfractal arrays. *IEEE Transactions on Antennas and Propagation* **56**, 97–107.

192. **Chen WL, Wang GM and Zhang CX** (2008) Fractal-shaped switched-beam antenna with reduced size and broadside beam. *Electronics Letters* **44**, 1110–1111.

193. **Petko JS and Werner DH** (2009) Interleaved ultrawideband antenna arrays based on optimized polyfractal tree structures. *IEEE Transactions on Antennas and Propagation* **57**, 2622–2632.

194. **Spence TG, Werner DH and Carvajal JN** (2010) Modular broadband phased-arrays based on a nonuniform distribution of elements along the Peano-Gosper space-filling curve. *IEEE Transactions on Antennas and Propagation* **58**, 600–604.

195. **Siakavara K** (2010) Hybrid-fractal direct radiating antenna arrays with small number of elements for satellite communications. *IEEE Transactions on Antennas and Propagation* **58**, 2102–2106.

196. **Gregory MD, Petko JS, Spence TG and Werner DH** (2010) Nature-inspired design techniques for ultra-wideband aperiodic antenna arrays. *IEEE Antennas and Propagation Magazine* **52**, 28–45.

197. **Spence TG and Werner DH** (2010) Generalized space-filling Gosper curves and their application to the design of wideband modular planar antenna arrays. *IEEE Transactions on Antennas and Propagation* **58**, 3931–3941.

198. **Kuzu S and Akcam N** (2017) Array antenna using defected ground structure shaped with fractal form generated by Apollonius circle. *IEEE Antennas and Wireless Propagation Letters* **16**, 1020–1023.

199. **El-Khamy SE, Eltrass AS and El-Sayed HF** (2018) Design of thinned fractal antenna arrays for adaptive beam forming and side lobe reduction. *IET Microwaves Antennas and Propagation* **12**, 435–444.

200. **Sanchez DA** (2008) *Multiband Integrated Antennas for 4G Terminals.* Boston, London: Artech House.

201. **Alibakhshikenari M, Virdee BS, See CH, Abd-Alhameed R, Ali AH, Falcone F and Limiti E** (2018) Study on isolation improvement between closely packed patch antenna arrays based on fractal metamaterial electromagnetic bandgap structures. *IET Microwaves Antennas and Propagation* **12**, 2241–2247.

Anirban Karmakar has received Ph.D. in Engineering from Jadavpur University, Kolkata, India, in 2015. He has more than 13 years of teaching experience and is currently holding the post of Assistant Professor in the Department of Electronics & Communication Engineering at Tripura University (A Central University), India. He has almost 40 research articles in refereed journals and international conference proceedings. He has served as a reviewer in different international journals. He was awarded the best paper award from different international conferences. He is a Senior Member of IEEE and has organized different workshops in the capacity of a convener and completed various funded projects received from UGC. Currently four research scholars are pursuing Ph.D. under his guidance. His areas of interest include planar and fractal wideband antennas, arrays, circular polarized antennas, DRA, etc.